Characterization of humoral and SARS-CoV-2 specific T cell responses in people living with HIV

Aljawharah Alrubayyi[1]†, Ester Gea-Mallorquí[1]†, Emma Touizer[2]†, Dan Hameiri-Bowen[1], Jakub Kopycinski[1], Bethany Charlton[1], Natasha Fisher-Pearson[1], Luke Muir[2], Annachiara Rosa[3], Chloe Roustan[3], Christopher Earl[3], Peter Cherepanov[3], Pierre Pellegrino[4], Laura Waters[4], Fiona Burns[5,6], Sabine Kinloch[6], Tao Dong[1], Lucy Dorrell[1], Sarah Rowland-Jones[1], Laura E. McCoy[2]†*, Dimitra Peppa[1,4]†*

Affiliations:

[1] Nuffield Dept of Clinical Medicine, University of Oxford, United Kingdom

[2] Division of Infection and Immunity, University College London, London, United Kingdom

[3] Chromatin Structure and Mobile DNA Laboratory, The Francis Crick Institute, London, United Kingdom

[4] Mortimer Market Centre, Department of HIV, CNWL NHS Trust, London, United Kingdom

[5]Institute for Global Health UCL, London, United Kingdom

[6]Royal Free London NHS Foundation Trust, London, United Kingdom

† These authors contributed equally

Corresponding authors: Dimitra.peppa@ndm.ox.ac.uk; l.mccoy@ucl.ac.uk

One Sentence Summary: Adaptive immune responses to SARS-CoV-2 in the setting of HIV infection

Abstract

There is an urgent need to understand the nature of immune responses generated against SARS-CoV-2, to better inform risk-mitigation strategies for people living with HIV (PLWH). Although not all PLWH are considered immunosuppressed, residual cellular immune deficiency and ongoing inflammation could influence COVID-19 disease severity, the evolution and durability of protective memory responses. Here, we performed an integrated analysis, characterizing the nature, breadth and magnitude of SARS-CoV-2-specific immune responses in PLWH, controlled on ART, and HIV negative subjects. Both groups were in the convalescent phase of predominately mild COVID-19 disease. The majority of PLWH mounted SARS-CoV-2 Spike- and Nucleoprotein-specific antibodies with neutralizing activity and SARS-CoV-2-specific T cell responses, as measured by ELISpot, at levels comparable to HIV negative subjects. T cell responses against Spike, Membrane and Nucleocapsid were the most prominent, with SARS-CoV-2-specific CD4 T cells outnumbering CD8 T cells. Notably, the overall magnitude of SARS-CoV-2-specific T cell responses related to the size of the naive CD4 T cell pool and the CD4:CD8 ratio in PLWH, in whom disparate antibody and T cell responses were observed. Both humoral and cellular responses to SARS-CoV-2 were detected at 5-7 months post-infection, providing evidence of medium-term durability of responses irrespective of HIV serostatus. Incomplete immune reconstitution on ART and a low CD4:CD8 ratio could, however, hamper the development of immunity to SARS-CoV-2 and serve as a useful tool for risk stratification of PLWH. These findings have implications for the individual management and potential effectiveness of vaccination against SARS-CoV-2 in PLWH.

Introduction

The global outbreak of severe acute respiratory syndrome coronavirus 2 (SARS-CoV-2), causing COVID-19 disease, has resulted in an overall 3% case fatality rate, posing unprecedented healthcare challenges around the world (Guan et al. 2020). With an evolving pandemic, urgent and efficient strategies are required for optimised interventions especially in patient populations with underlying chronic diseases. Nearly 40 million people are living with HIV (PLWH) worldwide and almost half of PLWH in Europe are over the age of 50 (Harris et al. 2018). However, due to scarcity of data it remains unknown whether antiviral responses to SARS-CoV-2 are compromised and/or less durable in PLWH following primary infection. Such knowledge is crucial in the future clinical management of PLWH during the course of the pandemic and for informing strategies for vaccination programmes.

Epidemiological evidence indicates that the risk of severe COVID-19 disease increases with age, male gender, and in the presence of comorbidities (Williamson et al. 2020; Wu and McGoogan 2020). PLWH, despite efficient virological suppression on antiretroviral treatment (ART), experience an increased burden of comorbid conditions associated with premature ageing (De Francesco et al. 2019; Guaraldi et al. 2011). These multi-morbidities are driven by residual inflammation on ART and ongoing immune dysregulation (Deeks and Phillips 2009) that could influence COVID-19 disease severity, the durability of protective antiviral responses, which may prevent future re-infection, and responsiveness to vaccination (Moir and Fauci 2017; Pallikkuth et al. 2012). Although there is no evidence of increased rates of COVID-19 disease among PLWH compared to the general population, mortality estimates vary between studies, with disparities in social health determinants and comorbidities likely having an influence (Bhaskaran

et al. 2021; Blanco et al. 2020; Boulle et al. 2020; Cooper et al. 2020; Geretti et al. 2020; Inciarte et al. 2020; Sigel et al. 2020). More recently, cellular immune deficiency and a lower CD4 T cell count/low CD4 T cell nadir have been identified as potential risk factors for severe SARS-CoV-2 infection in PLWH, irrespective of HIV virological suppression (Hoffmann et al. 2020). Burgeoning evidence supports a role for CD4 T cells in the control and resolution of acute SARS-CoV-2 infection (Oja et al. 2020; Rydyznski Moderbacher et al. 2020; Tan et al. 2021), in addition to providing CD8 T cell and B cell help for long-term immunity (Crotty 2015; Laidlaw et al. 2016). Any pre-existing CD4 T cell depletion in PLWH, as described in patients with haematological malignancy (Annika Fendler 2020), could therefore be a potential driver of dysregulated immunity to SARS-CoV-2, hampering antiviral responses (Calvet et al. 2020) and development of immunological memory.

Despite the collective efforts to define the correlates of immune protection and evaluate the durability of protective immune responses elicited post SARS-CoV-2 infection in the general population, reports in PLWH are limited. Overall, the majority of people infected with SARS-CoV-2 in the absence of HIV develop durable antibody responses including neutralizing antibodies and T cell responses (Dan et al. 2020; Ripperger et al. 2020; Rydyznski Moderbacher et al. 2020; Seow et al. 2020; Wajnberg et al. 2020). In most cases the magnitude of humoral responses is complemented by multi-specific T cell responses and appears to be dependent on the severity and protracted course of COVID-19 disease (Robbiani et al. 2020; Rydyznski Moderbacher et al. 2020; Wajnberg et al. 2020). However, humoral and cellular immune responses are not always correlative, with T cell immunity being induced even in the absence of detectable antibodies during mild COVID-19 disease (Reynolds et al. 2020; Rydyznski

Moderbacher et al. 2020; Sekine et al. 2020) and predicted to be more enduring from experience with other coronaviruses (Le Bert et al. 2020; Ng et al. 2020). Notably, older individuals more often display poorly co-ordinated immune adaptive responses to SARS-CoV-2 associated with worse disease outcome (Rydyznski Moderbacher et al. 2020; Sattler et al. 2020). This is particularly pertinent for PLWH, in whom the combined effect of ageing/premature immunosenescence and residual immune dysfunction in the era of effective of ART could have important consequences for the development of immune responses to a new pathogen and vaccination (George et al. 2015). To date, a single case report suggests a longer disease course and delayed antibody response against SARS-CoV-2 in HIV patients (Wang et al. 2020), but a simultaneous assessment of antibodies and T cell responses in the convalescent phase of COVID-19 disease is lacking in PLWH.

To address this knowledge gap, we performed an integrated cross-sectional analysis of different branches of adaptive immunity to SARS-CoV-2 in PLWH, controlled on ART, compared to HIV negative individuals recovered from mainly non-hospitalized mild COVID-19 disease. Our data reveal an association between the magnitude of SARS-CoV-2 T cell responses and the CD4:CD8 ratio in PLWH, in whom a decreased representation of naïve CD4 T cell subsets could potentially compromise protective immunity to SARS-CoV-2 infection and/or vaccination.

Results

COVID-19 cohort

Forty-seven individuals with HIV infection, well controlled on ART (for >2 years) with an undetectable HIV RNA, were recruited for this study during a defined period of time between

July 2020 and November 2020. Of these donors, twenty four previously had laboratory confirmed SARS-CoV-2 diagnosis (RT-PCR+ and/or Ab positive) with a median days post-symptom onset (DPSO) of 148 days; twenty three were probable/possible cases with a higher median DPSO of 181 days. The majority had ambulatory mild COVID-19 disease not requiring hospitalization (score 1-2 on WHO criteria). Eight subjects out of the laboratory confirmed cases had moderate disease requiring hospitalization (score 4-5 on WHO criteria). The ages of the subjects ranged from 30-73 years of age (median 52 years old) and were predominately White Caucasian males. The cohort included donors capturing a range of CD4 counts (133-1360) and CD4:CD8 ratios (0.17-2.54), reflective of the different lengths of HIV infection/CD4 T cell nadir and variable levels of immune reconstitution post treatment. As a comparator group we sampled thirty five HIV seronegative health care workers (HCW), thirty one with laboratory confirmed SARS-CoV-2 diagnosis and four suspected/household contacts of a confirmed case. The HCW group had a mild course of COVID-19 disease sampled at a similar median DPSO, with four donors recruited in the convalescent phase post moderate disease (score 4-5 on WHO criteria). HIV negative subjects were younger in age (range 26-65; median 41) with a more equal female:male distribution (**Table S1**). A group of HIV positive (n=16) donors with samples stored prior to the pandemic, matched to the HIV cohort recovered from COVID-19 disease, was used as controls. Inter-experimental variability was minimized by running matched cryopreserved samples in batches with inter-assay quality controls. Further details on patients' characteristics and comorbidities are included in **Table S1**.

Levels of SARS-CoV-2 antibodies in the study groups

ELISA was used to screen plasma samples for antibodies against the external Spike antigen, using immobilized recombinant Spike $S1_{1-530}$ subunit protein (S1), and against immobilized full-length internal Nucleoprotein (N) antigen to confirm prior infection as previously described (Ng et al. 2020; O'Nions et al. 2021; Pickering et al. 2020) (**Fig. 1A**). A sample absorbance greater than 4-fold above the average background of the assay was regarded as positive, using a threshold established with pre-pandemic samples (**Fig. S1A, B**) and as previously described (Pickering et al. 2020). The screening assay, followed by titer quantification (based on an in-assay standard curve) (O'Nions et al. 2021), demonstrated that 95.8% (23/24) of individuals from the HIV positive group with prior laboratory confirmed COVID-19 and 30.43% (7/23) with suspected disease, during the first wave of the pandemic, had measurable titers for SARS-CoV-2 S1 and N sampled at a median 146 DPSO (DPSO range 46-232) and 181 DPSO (range 131-228), respectively (**Fig. 1A-C**). Similarly, in the HIV negative group with laboratory confirmed COVID-19 disease, 93.5% (29/31) had detectable SARS-CoV-2 antibodies to S1 and N at 146 DPSO (101-220), whereas none of the suspected/household contacts in this group (0/4) had quantifiable titers (DPSO median 200; range 125-203) (**Fig. 1A-C**). S1 and N titers were found to be comparable between the HIV positive and negative groups (**Fig. 1B, C**) and correlated with one another, although levels were heterogenous among donors as previously observed (**Fig. 1D**).

To determine whether the SARS-CoV-2 antibodies generated are able to inhibit SARS-CoV-2 infection, we employed a serum neutralisation assay with pseudotyped SARS-CoV-2, to calculate the 50% inhibitory serum dilution (ID50) (Seow et al. 2020). Overall, we detected similar neutralization levels (**Fig. 1E**) and comparable profiles across the two study groups in terms of the number of individuals with high potency, low potency or no neutralizing activity

(<50 ID50) (**Fig. 1F**), which correlated with anti-S1 IgG levels (**Fig. 1G**). A range of neutralizing antibodies (nAb) was detected in the groups, with some samples exhibiting strong neutralization despite low S1 titers irrespective of disease severity (**Fig. 1G**).

No association was observed between S1 binding titers, age and gender in the two groups (**Fig. S1C**). A weak positive correlation was seen between neutralization levels and age according to male gender in the HIV positive group, where subjects were older and females were notably under-represented (**Fig. S1D**). Neutralization levels did not correlate with DPSO (**Fig. S1E**) and were detectable up to 7 months post infection. No clear association was observed according to ethnicity (**Fig. S1F**). Together these results show no significant differences in the IgG-specific antibody response to SARS-CoV-2 and neutralization capacity according to HIV status after recovery from COVID-19 disease. These findings should be considered in the context of this cohort in which the majority of cases were mild and therefore may not reflect the full burden of disease associated with SARS-CoV-2 infection.

SARS-CoV-2 multi-specific T cell responses

The presence of T helper 1 (Th1) immunity has been described in a number of studies investigating T cell-specific immune responses to SARS-CoV-2 infection in various phases of the infection. We therefore initially assessed global SARS-CoV-2 T cell frequencies by IFN-γ-ELISpot using overlapping peptide (OLP) pools to detect T cell responses and cumulative frequencies directed against defined immunogenic regions, including Spike, Nucleocapsid (N), membrane (M), Envelope (Env), and open reading frame (ORF)3a, ORF6, ORF7 and ORF8 (**Fig. 2A**). Out of the 30 HIV positive and 30 HIV negative individuals (including previously

laboratory confirmed cases and additional subjects found to be SARS-CoV-2 seropositive on screening), the majority of donors in each group had a demonstrable cellular response directed predominately against Spike and N/M. Responses to accessory peptide pools (ORFs) and the structural protein Env were less frequent and significantly lower to other antigens observed, irrespective of HIV status (**Fig. 2B and Fig. S2A, B**). The overall magnitude of responses against Spike, M and N did not differ significantly between the groups (**Fig. 2C**). In HIV positive donors the cumulative SARS-CoV-2 responses across all pools tested were lower in magnitude compared to that of T cells directed against well-defined CD8 epitopes from Influenza, Epstein Barr Virus (EBV) and Cytomegalovirus (CMV)-(FEC pools) tested in parallel within the same donors, but higher compared to HIV-gag responses (**Fig. 2D**). By contrast, responses to FEC pools were comparable in magnitude to the cumulative SARS-CoV-2-specific T cell responses detected in the HIV negative donors, likely reflecting the lower CMV seropositivity in the HIV negative group compared to the HIV positive group (54.28% CMV seropositive versus 97.87% CMV seropositive, respectively) (**Fig. 2D**). In line with previous studies we observed a wide breadth and range of cumulative SARS-CoV-2 T cell frequencies, with over 90% of donors in each group showing a response (**Fig. 2E, F**) (Grifoni et al. 2020; Peng et al. 2020; Reynolds et al. 2020). However, the proportion of HIV positive and negative donors with T cell responses to individual SARS-CoV-2 pools within given ranges varied, with a higher percentage of HIV positive donors having low level responses **(Fig. 2G).**

Responses to Spike, M and N peptide pools were significantly higher in donors with confirmed SARS-CoV-2 infection compared to subjects with no evidence of infection who displayed relatively weak responses; small responses were also noted in a proportion of HIV positive

subjects with available pre-pandemic samples (**Fig. S2C**). Additional work is required to investigate potential cross-reactive components of these responses with other human coronaviruses, as has been reported in other studies (Braun et al. 2020; Grifoni et al. 2020; Le Bert et al. 2020; Sekine et al. 2020). These data were derived from cryopreserved samples, which may underestimate the magnitude of the detected responses (Owen et al. 2007).

Given the considerable heterogeneity in the magnitude of the observed responses in both groups, we related these to HIV parameters, age, gender and DPSO. We detected a positive correlation between CD4:CD8 ratio and summed total responses to OLP pools against SARS-CoV-2 in HIV positive subjects (r=0.3820, p=0.037) **(Fig. 2H)**; this relationship was similar for N (r=0.4282, p=0.018) and stronger for responses against M (r=0.4853, p=0.007) **(Fig. S2D-E).** These data suggest that, despite effective ART, incomplete immune reconstitution may potentially impact on the magnitude of T cell responses to SARS-CoV-2. Previous observations have demonstrated an association between SARS-CoV-2-specific T cells, age and gender, with T cell immunity to Spike increasing with age and male gender in some studies (Reynolds et al. 2020). Despite an older age and male predominance in our HIV cohort we did not detect any association between ELISpot responses to Spike and donor age (**Fig. S2F-G**). There was no correlation between DPSO and T cells directed either against Spike or total responses against SARS-CoV-2. These responses were nonetheless detectable up to 232 DPSO (median 151 range 46-232) in HIV positive subjects, and similarly in HIV negative donors (median 144; range 101-220) (**Fig. S2H-I**). Given that the majority of the donors, in both groups, experienced mild COVID-19 disease, any associations between the magnitude of responses and disease severity are limited. No

differences were observed in the magnitude of T cell responses according to ethnicity and gender, irrespective of HIV status (**Fig. SJ-K**).

T cell and antibody response complementarity

Next, we compared T cell responses, antibody levels and nAb responses in individual donors to better understand any complementarity between humoral and cellular responses detected by IFN-γ-ELISpot. SARS-CoV-2-specific T cell responses correlated with antibody binding titers in the HIV negative group (**Fig. 3A, C**). Although the majority of HIV positive subjects had detectable antibody and T cell responses to SARS-CoV-2, the magnitude of the cellular immune responses correlated weakly only with N IgG binding titers but not with S1 IgG binding titers (**Fig. 3B, D**). These data suggest that T cell and antibody responses are not always concordant, implying that the binding titer is not always a good predictor of the magnitude of the T cell response, especially in PLWH. Nonetheless, in some instances, despite low level or lack of detectable S1-binding IgG, a strong T cell response to SARS-CoV-2 was demonstrable, suggesting a degree of compensation between branches of adaptive immunity.

We subsequently examined neutralization ID50 values for individual donors in relation to T cell responses to individual SARS-CoV-2 antigen pools and summed responses. In HIV negative donors a correlation was observed between T cell responses to Spike protein and ID50 ($r = 0.4002$, $p = 0.0315$), with donors lacking a response to Spike generally maintaining low-frequency T cell responses to other specificities. When cumulative responses were ranked by the magnitude of nAb response, a single HIV negative donor with an ID50>1000 had no detectable SARS-CoV-2-specific T cells (**Fig. 3E**). In HIV positive donors no correlation was detected

between neutralization capacity and responses to individual SARS-CoV-2 peptides or pooled responses. A single HIV positive donor (1/29) with undetectable neutralization activity, and another donor with potent neutralization (>1000), had no measurable T cell response to any of the pools tested (**Fig. 3F**).

SARS-CoV-2 specific T cell responses are dominated by CD4 T cells

Following the initial broad screening of the antiviral responses to SARS-CoV-2, intracellular cytokine staining (ICS) was used to assess the composition and polyfunctionality of T cell responses in a group of HIV positive (n=11) and HIV negative (n=12) donors with available PBMC and detectable responses by IFN-γ-ELISpot. To determine the functional capacity of SARS-CoV-2-specific CD4 and CD8 T cells, we stimulated PBMCs with overlapping Spike, M and N (non-Spike) peptide pools, in addition to CMV pp65 and HIV gag peptides within the same individuals. We focused on Spike, M and N as these antigens dominated responses detected by ELISpot. Expression of the activation marker CD154 and production of IFN-γ, IL-2 and TNF-α were measured as functional readouts (**Fig. 4A)**. SARS-CoV-2-specific CD4 T cells directed against Spike and non-Spike (M/N) predominantly expressed CD154 alone or in combination with IL-2, TNF-α and IFN-γ, consistent with a Th1 profile, and these aggregated responses were comparable between the groups (**Fig. 4A, B**). SARS-CoV-2-specific CD4 T cells exhibited polyfunctional responses, with T cells expressing up to three cytokines (**Fig. 4C**). We detected no significant differences in CD4 T cell responses, according to cytokine profile, to individual pools directed against Spike, M and N in the two groups (**Fig. 3C and Fig. S3A**). Aggregated CD4 T cell responses against all SARS-CoV-2 pools tested were higher compared to CMV-specific responses and HIV-gag responses within the same donors (**Fig. S3D, E**).

SARS-CoV-2-specific CD8 T cells largely expressed IFN-γ alone or in combination with TNF-α, exhibiting a different cytokine profile to CD4 T cells as expected (**Fig. 4D**). A trend toward lower mean aggregated CD8 T cell responses and polyfunctionality against Spike relative to non-Spike was observed in HIV negative individuals (**Fig. 4D, E, F**). Although SARS-CoV-2-specific CD8 T cell responses did not differ significantly between the two groups, mean response frequency was lower in HIV positive individuals against non-Spike pools (**Fig. 4E**). When we examined the individual cytokine profile, depending on antigen specificity, IL-2 production was reduced in CD8 T cells targeting non-Spike pools in HIV positive individuals compared to HIV negative donors (**Fig. S3F-H**). The proportion of CD8 T cells specific for CMV was higher compared to SARS-CoV-2-specific CD8 T cells irrespective of HIV status and similar to HIV-gag responses (**Fig. S3I and J**). Notably, SARS-CoV-2-specific CD8 T cells against Spike and non-Spike pools were less frequent, with CD4 T cells similarly outnumbering CD8 T cells regardless of HIV status (**Fig. 4G**). Total SARS-CoV-2-specific CD4 T cell responses correlated with the magnitude of T cell responses detected by ELISpots and with neutralization titers in the same individuals when data from HIV positive and negative donors were combined **(Fig. 4H, I).** This association was also seen between Spike and non-Spike-specific CD4 T cells detected via ICS and overall T cell responses against Spike/non-Spike detected via ELISpots ($r=0.5734$, $p=0.0042$ and $r=0.4852$, $p=0.0189$ respectively), indicating that CD4 T cells are the dominant population responding to SARS-CoV-2.

In line with previous observations, we found that SARS-CoV-2-specific T cells predominately display an effector memory (EM) and/or a terminally differentiated effector memory (TEMRA)

cell phenotype for CD4 and CD8 T cells respectively (**Fig. 5A-D**) (Breton et al. 2020; Dan et al. 2020). Previous studies have suggested that higher expression of programmed cell death-1 (PD-1) on T cells in COVID-19 patients could signify the presence of exhausted T cells (De Biasi et al. 2020; Song et al. 2020; Zheng et al. 2020). We therefore examined the expression of PD-1 in relation to activation and function among SARS-CoV-2-specific CD4 T cells. The proportion of CD154+ IFN-γ producing cells was significantly higher in PD-1^{+} cells compared to PD-1^{-} cells regardless of HIV serostatus, likely reflecting activated functional cells rather than exhausted populations (**Fig. 5E**) (Rha et al. 2021). An inverse correlation between the expression of PD-1 expressing SARS-CoV-2-specific CD4 T cells and DPSO was observed in HIV negative donors (**Fig. 5F**).

Immune profile relationships between convalescent HIV positive and negative individuals

During COVID-19 disease, excessive activation of T cells can lead to lymphopenia, including altered subset distribution and function, and these alterations can persist into convalescence (Breton et al. 2020; Chen and John Wherry 2020; De Biasi et al. 2020; Mathew et al. 2020). This prompted us to further evaluate changes in the T cell compartment and the relationship between antigen-specific T cells and antibodies with individual T cell parameters and immunological metrics in our cohort. To this end we utilized a broad immunophenotyping flow cytometry panel to capture major cell types.

Global t-distributed stochastic neighbour embedding (t-SNE) high dimensional analysis demonstrated significant alterations in the T cell compartment between HIV negative and positive individuals recovered from COVID-19 (**Fig. 6A**). Lower proportions of circulating CD4

T cells and higher proportions of CD8 T cells were confirmed by traditional gating in HIV infected individuals recovered from COVID-19 disease compared to HIV negative individuals (**Fig. 6B**). Consistent with alterations described in HIV infection (L. Zhang et al 1999, M.D. Hazenberg et al 2000, D.C. Douek 1998), naïve T cell frequency was reduced in SARS-CoV-2 convalescent HIV positive donors compared to HIV negative subjects. This was accompanied by higher proportions of terminally differentiated effector memory (TEMRA: $CD45RA^{+}CCR7^{-}$) within the total CD8 T cell population in HIV infected individuals, contributing to an altered representation of naïve/memory T cells (Roederer et al. 1995) (**Fig. 6C**). Notably, the percentage of naïve CD4 T cells correlated with the CD4:CD8 ratio and SARS-CoV-2-specific T cell responses in HIV positive donors (**Fig. 6D, E**), suggesting that the scarce availability of naïve CD4 T cells could influence the extent/magnitude of the T cell response to SARS-CoV-2 infection. Recent data have demonstrated a link between naïve CD4 T cells, age and COVID-19 disease severity in older individuals (Rydyznski Moderbacher et al 2020). Whereas naïve CD8 and CD4 T cells correlated with age in HIV negative donors, this relationship between age and naïve T cells was lost in HIV infected donors (**Fig. 6F-I**). Together these observations suggest that altered T cell homeostasis and likely premature immunosenescence in HIV infection could compromise T cell mediated responses to a new pathogen (Douek et al. 1998).

Previous work focusing on markers of activation/exhaustion to evaluate the T cell compartment during the acute and convalescent phase of SARS-CoV-2 infection, has demonstrated lasting changes (Breton et al. 2020). Such information is lacking in the setting of HIV infection, normally characterised by persistent immune activation together with cell alterations and T cell exhaustion (Breton et al. 2013; El-Far et al. 2008). The proportion of T cells co-expressing

344 HLADR/CD38 and PD-1/TIGIT (T cell immunoreceptor with Ig and ITIM domains) in HIV
345 infected individuals was significantly higher when compared with HIV negative donors but did
346 not correlate with virus-specific parameters (**Fig. S4A-D).**
347
348 Circulating T follicular helper (cTfh) cells represent a substantial proportion of the SARS-CoV-
349 2-specific T cells in acute and convalescent infection (Rodda et al. 2021; Rydyznski
350 Moderbacher et al. 2020), and are required for maturation and development of B cell responses
351 in germinal centres and the induction of IgG production (Crotty 2015). A close association
352 between cTfh cells and the virus-specific antibody production in the convalescent phase of
353 COVID-19 disease has been described (Zhang et al. 2021). We detected elevated frequencies of
354 cTfh (CXCR5+PD-1+) HIV infected subjects compared to HIV infected donors, however, no
355 correlation was observed with antibody levels (**Fig. S4E, F**). Whether further quantitative and
356 qualitative differences exist between cTfh cell subsets in HIV positive (Pallikkuth et al. 2017)
357 and negative individuals that could alter their capacity to instruct B cells and influence responses
358 to SARS-CoV-2 infection merits further investigation in larger cohorts.
359

360 **Discussion**

361 The COVID-19 pandemic is causing much global uncertainty, especially for people with pre-
362 existing medical conditions such as PLWH. In this study, we aimed to bridge the knowledge
363 gaps in our understanding of the specificity, magnitude and duration of immunity to SARS-CoV-
364 2 in this patient group, which is critical for tailoring current and future mitigation measures,
365 including vaccine strategy. This integrative analysis demonstrates that the majority of PLWH

366 evaluated in the convalescent phase from mild COVID-19 disease can mount a functional
367 adaptive immune response to SARS-CoV-2.
368
369 Most PLWH developed S1/N-reactive and neutralizing antibody responses similar to HIV
370 negative donors in our study and similar to observations reported in the general population at
371 least five months after primary infection (Gaebler et al. 2020; Reynolds et al. 2020) (Seow et al.
372 2020). Circulating SARS-CoV-2 neutralizing antibody titers were, however, low in a fraction of
373 recovered COVID-19 cases (Dan et al. 2020; Robbiani et al. 2020; Seow et al. 2020; Wajnberg
374 et al. 2020), indicating that either the serum concentration/neutralizing antibody potency was
375 suboptimal or, more likely, that an earlier response could have waned by the time of sampling at
376 DPSO as previously observed (Seow et al. 2020). Some samples in both groups showed strong
377 neutralization despite low anti-S1 binding titers, suggesting the possibility of the presence of
378 neutralizing antibodies directed against other viral epitopes and/or greater production of non-
379 neutralizing antibodies, or a role of other isotypes in neutralizing responses. It should be noted
380 that our data reflect those who recovered from mostly mild COVID-19 disease, limiting our
381 conclusions about disease associations. Whether seroconversion rates and kinetics of antibody
382 responses differ according to HIV status need to be addressed in longitudinal studies from acute
383 infection or vaccination into convalescence. While the exact duration of immunity conferred by
384 natural infection remains unresolved, induction of neutralizing antibodies and presence of
385 antibodies to SARS-CoV-2 is thought to confer a degree of protection against SARS-CoV-2
386 (Anderson et al. 2020; Folegatti et al. 2020; Lumley et al. 2020; Polack et al. 2020; V Hall 2020;
387 Yu et al. 2020).
388

389 In addition to antibodies, CD4 T cells and CD8 T cells can provide protective roles in controlling
390 SARS-CoV-2 infection (Altmann and Boyton 2020; Kim et al. 2020), with T cell immunity
391 potentially being more enduring, as in the case of SARS-CoV (Le Bert et al. 2020; Tang et al.
392 2011). In keeping with the published literature, we detected T cell responses via IFN-γ-ELISpot
393 in the majority of HIV positive and negative donors. In both groups these responses were
394 variable in magnitude and predominately targeted Spike, M and N, with smaller responses to
395 regions of the viral proteome tested being detected, consistent with previous studies (Grifoni et
396 al. 2020; Peng et al. 2020; Reynolds et al. 2020).
397
398 Notably, a positive association was observed between the CD4:CD8 ratio in HIV infected
399 subjects and the magnitude of T cell responses against SARS-CoV-2. This suggests that some
400 PLWH with residual immune perturbations, despite effective virological suppression on ART,
401 may generate suboptimal T cell memory responses. With emerging information on PLWH with
402 COVID-19 disease, a more pronounced immunodeficiency, defined as a current CD4 count
403 <350/μL and a low CD4 nadir, has been associated with an increased risk for severe COVID-19
404 disease and mortality. With modern ART and successful viral suppression, absolute CD4 count
405 (despite normalisation) may not accurately reflect the extent of immunological alterations that
406 could persist in HIV infected individuals on treatment (Opportunistic Infections Project Team of
407 the Collaboration of Observational et al. 2012). A low or inverted CD4/CD8 ratio is considered
408 an immune risk phenotype associated with altered immune function, immunosenescence and
409 chronic inflammation in both HIV positive and negative populations (Appay and Sauce 2008;
410 Serrano-Villar et al. 2014a; Serrano-Villar et al. 2014c). Due to its predictive power for adverse
411 clinical outcomes in HIV infection and in the ageing general population (Helleberg et al. 2015;

412 Serrano-Villar et al. 2014c; Serrano-Villar et al. 2014b), including its potential role as a
413 prognostic factor of COVID-19 disease severity (Calvet et al. 2020), the CD4:CD8 ratio could
414 represent an additional tool for risk stratification of PLWH. The relationship between naïve CD4
415 T cells, CD4:CD8 ratio and magnitude of SARS-CoV-2-specific responses in our cohort
416 highlights the dependency between new antigen-specific responses and the available pool of
417 naïve lymphocytes. Fewer pre-existing naïve CD4 T cells coupled with the relative
418 overrepresentation of memory CD8 T cells in the context of HIV, independent of age, could
419 exacerbate the clinical outcome of SARS-CoV-2 infection. These changes in the T cell
420 compartment can lead to reduced priming and poorly coordinated early and subsequent memory
421 immune responses to SARS-CoV-2. Our cohort and interim analysis does not represent the entire
422 spectrum of immune dysfunction, which we will continue to probe through ongoing recruitment
423 to test these relationships more rigorously. This would be highly relevant in the context of
424 emergence of specific SARS-CoV-2 variants associated with immunosuppression described in
425 the UK (SA Kemp 2020), and in parts of the world with high HIV prevalence and suboptimal
426 HIV suppression levels (Houriiyah Tegally 2020).
427
428 In agreement with other studies, our data show that in individuals with detectable cellular
429 responses, CD4 T cell responses to SARS-CoV-2 Spike and non-Spike antigens are more
430 common than CD8 T cell responses (Grifoni et al. 2020; Sekine et al. 2020; Zuo J 2020). This
431 could reflect a bias, from using peptide pools, towards MHC class II presentation and more
432 selective recognition by CD4 T cells (Grifoni et al. 2020). Preferential expansion of CD4 T cells
433 has been associated with control of primary SARS-CoV-2 infection (Rydyznski Moderbacher et
434 al. 2020) underscoring their relevance in PLWH with persistent alterations in their T cell

compartments. In a small group of donors, already found to be responsive via ELISpots, further evaluation of T cell polyfunctionality in response to SARS-CoV-2 Spike and non-Spike pools revealed similar profiles in SARS-CoV-2 CD4 T cells irrespective of HIV status. Given that contributions of T cells specific to any viral protein can be relevant for protective immunity, non-Spike proteins could also represent valuable components for future vaccine strategies. The reduced production of IL-2 from SARS-CoV-2-specific CD8 T cells in HIV infected donors could, however, hinder their proliferative potential and long-term immune memory post natural infection and/or immunization (Zimmerli et al. 2005). Together, these results provide further immunological context into the described associations between ongoing immunodeficiency and worse COVID-19 disease outcome, and the subsequent development of immune memory responses. Further work is required to comprehensively characterise the epitope repertoire elicited by SARS-CoV-2 infection in the context of a broad set of HLA alleles to define patterns of immunodominance.

Our data indicate that antibody and T cell responses in convalescent individuals with predominately mild disease can be uncoupled. The lack of correlation between Spike-specific T cells and S1 binding IgG titers and neutralization levels in HIV positive individuals could point toward impairment of Tfh cells (Pallikkuth et al. 2017), which make up a significant proportion of SARS-CoV-2-specific cells (Boppana et al. 2020; Juno et al. 2020). The observed disparity of T cell and antibody responses in certain individuals could also reflect differences in early innate immune responses potentially resulting in dysregulated priming and incongruent T and B cell responses (Zhou et al. 2020). However, this remains to be determined.

458 There are limitations to this study. The observed heterogeneity in the magnitude of cellular and
459 humoral responses that are not always fully coordinated highlights the need to consider
460 additional putative factors as they relate to adaptive immunity. This cross-sectional study was not
461 powered to study age and demographic differences according to the full spectrum of COVID-19
462 disease by HIV serostatus. Larger studies are required to determine the role of gender, racial and
463 ethnicity effects, especially in areas of high HIV burden and additional comorbidities, to help
464 identify individuals who are particularly vulnerable to the impact of SARS-CoV-2 infection and
465 need targeted vaccination interventions. Nonetheless, the prospective, longitudinal design of this
466 current study, integrating clinical parameters, antibody and T cell responses, will help address
467 longer term protective immunity and emerging questions, such as immune responses to new
468 SARS-CoV-2 variants (C Rees-Spear 2021; Houriiyah Tegally 2020; SA Kemp 2020; Sandile
469 Cele 2021; Wibmer et al. 2021), and during the subsequent vaccination roll-out.
470
471 Collectively, our results provide benchmark data into the facets of adaptive immunity against
472 SARS-CoV-2 in the setting of treated HIV infection, providing evidence for medium-term
473 durable antibody and cellular responses. Although reassuring, our data also have implications for
474 PLWH with inadequate immune reconstitution, reflected in the low/inverted CD4:CD8 ratio, and
475 potentially decreased ability to respond to SARS-CoV-2. This subpopulation of PLWH may be
476 more vulnerable to circulating virus with relevance to vaccine prioritization and potential
477 effectiveness. In the era of ART, CD4:CD8 ratio, should be considered as a readily accessible
478 biomarker for assessing individual risks in PLWH, a proportion of whom may require tailored
479 vaccine strategies to achieve long-term protective immunity.
480

Materials and Methods

Ethics statement

The protocols for the human study were approved by the local Research Ethics Committee (REC) – Berkshire (REC 16/SC/0265). The study conformed to the Helsinki declaration principles and Good Clinical Practice (GCP) guidelines and all subjects enrolled into the study provided written informed consent.

Study Subjects

HIV seronegative adults (>18 years of age, comprising hospital-based healthcare workers) and chronically HIV infected patients (on antiretroviral treatment for at least 2 years with undetectable HIV RNA) with prior confirmed or suspected COVID-19 disease were recruited. All study participants were screen anti-Hepatitis C virus and anti HBsAg negative. Confirmed SARS-CoV-2 infection by SARS-CoV-2 PCR and/or Roche antibody tests was declared by the participants, who were asked to provide details on the timing and nature of symptoms. Additional demographic information and underlying medical conditions were captured on a health questionnaire. European Centre for Disease Prevention (ECDC) criteria were used for case definition for COVID-19 disease. Severity of COVID-19 disease was according to the WHO criteria. This is a cross-sectional analysis of baseline samples collected during the convalescent phase of SARS-CoV-2 infection as part of a prospective, observational longitudinal cohort study. A total of n=47 HIV positive and n=35 HIV negative subjects with recovered confirmed and/or suspected COVID-19 disease were included (**Table. S1 Subject characteristics**). Sixteen demographically age-, sex- and lifestyle-matched HIV-1 seropositive individuals were included for comparison, from whom sample were collected between (February

2017-November 2019; pre-pandemic). All participants were recruited at the Mortimer Market Centre for Sexual Health and HIV Research and the Royal Free Hospital (London, UK) following written informed consent as part of a study approved by the local ethics board committee. Clinical characteristics of participants are summarized in **Table. S1**. Further details in the exact number of subjects utilized for each assay are indicated in the figure legends and Results section.

Case definition for coronavirus disease 2019 (COVID-19), as of 03 December 2020 European Centre for Disease Prevention and Control [https://www.ecdc.europa.eu/en/covid-19/surveillance/case-definition]. Severity of COVID-19 was classified according to the WHO (World Health Organisation) clinical progression scale.

Peripheral blood mononuclear cells (PBMC) and Plasma Isolation

Whole blood from all participants was collected in heparin-coated tubes and stored at room temperature prior to processing. In brief, PBMCs were isolated by density gradient sedimentation. Whole blood was transferred to conical tubes and then centrifuged at 2000 rpm, at room temperature (RT) for 5-10 minutes. Plasma was then collected, aliquoted and stored at −80°C for further use. The remaining blood was diluted with RPMI (Corning, Manassas, VA, USA), layered over an appropriate volume of room temperature Histopaque (Histopaque-1077 Cell Separation Medium, Sigma-Aldrich, St. Louis, MO, USA), and then centrifuged for 20 min at 2000 rpm at room temperature without brake. After centrifugation, the PBMC layer was carefully collected, transferred to a conical tube and washed with RPMI. An aliquot of cells was stained with trypan blue and counted using Automated Cell Counter (Bio-Rad, Hercules, California, USA). Isolated PBMCs were then cryopreserved in a cryovial in cell recovery

freezing medium containing 10% Dimethyl Sulfoxide (DMSO) (MP Biomedicals, LLC, Irvine, CA, USA) and 90% heat inactivated fetal bovine serum (FBS) and stored at −80°C in a Mr. Frosty freezing container overnight before being transferred to liquid nitrogen for further storage.

Serum isolation

For serum isolation, whole blood was collected in serum separator tubes and stored briefly at room temperature prior sample processing. Serum tubes were centrifuged for 5 min at 2000 rpm, and then serum was collected, aliquoted and stored at −80°C for further use.

Semiquantitative ELISA for S1 and N

This assay is based on a previously described assay (O'Nions et al. 2021; Pickering et al. 2020; Seow et al. 2020). Briefly, 9 columns of a 96-half-well Maxisorp plate (Nalgene, NUNC International, Hereford, UK) were coated overnight at 4°C with 25 µl of S1 or N (gift from Peter Cherepanov, Crick Institute) purified protein at 3 µg/ml in PBS, the remaining 3 columns were coated with 25 µl goat anti-human F(ab)'2 (1:1,000) in PBS to generate an internal standard curve. The next day, plates were washed with PBS-T (0.05% Tween in PBS) and blocked for 1h at RT with assay buffer (5% milk powder PBS-T). Assay buffer was then removed and 25 µl of patient sera at dilutions from 1:50 – 1:1000 in assay buffer added to the antigen-coated wells in duplicate. Serial dilutions of known concentrations of IgG were added to the F(ab)'2 IgG-coated wells in triplicate. Following incubation for 2 hours at room temperature, plates were washed with PBS-T and 25 µl alkaline phosphatase-conjugated goat anti-human IgG (Jackson ImmunoResearch) at a 1:1000 dilution in assay buffer added to each well and incubated for 1 hour at room temperature. Plates were then washed with PBS-T, and 25µl of alkaline

phosphatase substrate (Sigma Aldrich) added. ODs were measured using a MultiskanFC (Thermofisher) plate reader at 405nm and S1 & N-specific IgG titers interpolated from the IgG standard curve using 4PL regression curve-fitting on GraphPad Prism 8.

Pseudovirus production and neutralization assays

HIV-1 particles pseudotyped with SARS-Cov-2 spike were produced by seeding $3x10^6$ HEK-293T cells in 10ml complete DMEM (DMEM supplemented with 10% FBS, L-Glutamine, 100 IU/ml penicillin and 100 µg/ml streptomycin) in a T-75 culture flask. The following day cells were transfected with 9.1 µg of HIV p8.91 packaging plasmid (Zufferey et al. 1997) , 9.1 µg of HIV-1 luciferase reporter vector plasmid (Seow et al. 2020), 1.4 µg of WT-SARS-CoV-2 spike plasmid (2) and 60 µg of PEI-Max (Polysciences). Supernatants were harvested 48h later, filtered through a 0.45 µm filter and stored at -80°C. Neutralization assays were performed on 96-well plates by incubating serial dilutions of patient serum with pseudovirus for 1h at 37°C 5% CO_2. HeLa ACE-2 cells (gift from James E Voss, Scripps Institute) were then added to the assay (10,000 cells per 100 µL per well). After 48/72h at 37°C 5% CO_2, supernatants were removed, and the cells were lysed; Brightglo luciferase substrate (Promega) was added to the plates and RLU read on a Glomax luminometer (Promega) as a proxy for infection. Measurements were performed in duplicate and fifty percent inhibitory dilution (ID50) values were calculated using GraphPad Prism 8.

IgG Purification

For individuals on ART, to avoid off-target neutralization due to the HIV pseudovirus backbone, we purified IgG from serum using Mini Bio-Spin Chromatography Columns (BioRad) by

incubating sera with a resin of protein G Sepharose beads (GE Healthcare) for 2h, eluting with 0.1M Glycine (pH 2.2) into 2M Tris-base, concentrating the IgG-containing fraction in a 50kD concentrator (Amicon, Merck) and quantifying the amount of IgG by Nanodrop. The purified IgG was serially diluted from 200 µg/ml in neutralization assays and the resulting ID50 calculated using the total IgG concentration of each serum sample prior to purification.

Standardized ELISA for measurement of CMV-specific IgG levels in plasma

The levels of CMV-specific IgG were measured using the Abcam Anti-Cytomegalovirus (CMV) IgG Human ELISA kit following manufacturer's instructions. Assays were run in duplicate and mean values per participant are reported in International Units (IU) per ml.

Phenotypic flow cytometric analysis

The fluorochrome-conjugated antibodies used in this study are listed in **Table. S2**. Briefly, purified cryopreserved PBMCs were thawed and rested for one hour at 37 °C in complete RPMI medium (RPMI supplemented with Penicillin-Streptomycin, L-Glutamine, HEPES, non-essential amino acids, 2-Mercaptoethanol, and 10% Fetal bovine serum (FBS)). Cells were then washed, resuspended in PBS, and surface stained at 4°C for 20 min with different combinations of antibodies in the presence of fixable live/dead stain (Invitrogen). Cells were then fixed and permeabilized for detection of intracellular antigens. The Foxp3 intranuclear staining buffer kit (eBioscience) was used according to the manufacturer's instructions for the detection of intranuclear markers. Samples were acquired on a BD Fortessa X20 using BD FACSDiva8.0 (BD Bioscience) and subsequent data analysis was performed using FlowJo 10 (TreeStar). Stochastic neighbor embedding (SNE) analysis was undertaken on the mrc.cytobank

platform to enable visualization of high-dimensional data in two-dimensional representations, avoiding the bias that can be introduced by manual gating of specific subsets (Amir el et al. 2013).

Peptide Pools:

For detection of virus-specific T cell responses, PBMCs were stimulated with the following peptide pools:

1. SARS-CoV-2 Spike: total of 15 to18-mers overlapping by 10 amino acid residues for Spike (S) synthesized using Two-dimensional peptide Matrix pools, divided into 16 "minipools" P1-P16 and grouped into pools S1 (P1-8) and S2 (P 9-16) (Peng et al. 2020).
2. SARS-CoV-2 Structural and accessory proteins: 15-mer peptides overlapping by 10 amino acid residues for Membrane protein (M) (Miltenyibiotec), Nucleocapsid (N) (Miltenyibiotec), Envelope (Env) protein and open reading frame (ORF) 3, 6, 7 (a kind gift from Tao Dong) (Peng et al. 2020)
3. Non-SARS-CoV-2 antigens: Peptide pools of the pp65 protein of human cytomegalovirus (CMV) (Miltenyibiotec, and NIH AIDS Reagent Repository), or HIVconsv peptide pools (NIH AIDS Reagent Repository) HIV-1 and Influenza HLA class I-restricted T cell epitope (ProImmune). CD8 T cell epitopes of human influenza, CMV and EBV viruses (namely FEC controls, NIH AIDS Reagent Repository) were used as positive controls.

Ex vivo IFN-γ ELISpot Assay

IFN-γ ELISpot assays were performed with cryopreserved isolated PBMCs as described previously (Peng et al. 2020). Briefly, ELISPOT plates (S5EJ044I10; Merck Millipore, Darmstadt, Germany) pre-wetted with 30 µl of 70% ethanol for a maximum of 2 minutes, washed with sterile PBS and coated overnight at 4 °C with anti–IFN-γ antibody (10 µg/ml in PBS; clone 1-D1K; Mabtech, Nacka Strand, Sweden). Prior to use, plates were washed with PBS and blocked with R10 (RPMI supplemented with Penicillin-Streptomycin, L-Glutamine, and 10% FBS) for 1 hour at 37 °C. The cells were plated at 2×10^5 cells/well for most of the participants or 1×10^5 cells/well for participants with lower cell recovery. Cells were cultured with overlapping peptide pools at 2 µg/ml or PHA (Sigma Aldrich, St Louis, MO) at 10 µg/ml as a positive control for 16-18 hours at 37 °C. Cells lacking peptide stimulation were used as a negative control. Plates were then washed four times with 0.05% Tween/PBS (Sigma-Aldrich) followed by two washes with PBS and then incubated for 2 hr at RT with biotinylated anti-IFN-γ (1 µg/mL; clone mAb-7B6-1; Mabtech). After six further washes, cells were incubated with alkaline phosphatase-conjugated streptavidin (Mabtech) at 1:1000 dilution for 1 hr at RT. Plates were then washed six times and developed using VECTASTAIN® Elite ABC-HRP according to the manufacturer's instructions (Mabtech). All assays were performed in duplicate. Spots were counted using an automated ELISpot Reader System (Autoimmun Diagnostika GmbH). Results are reported as difference in (Δ) spot forming units (SFU) per 10^6 PBMCs between the peptide-stimulated and negative control conditions. Responses that were found to be lower than two standard deviations of the sample specific control were excluded. An additional threshold was set at > 5 SFU/10^6 PBMCs, and results were excluded if positive control wells (PHA, FEC) were negative.

Intracellular cytokine stimulation (ICS) functional assay

ICS was performed as described previously (Gupta et al. 2019). Briefly, purified PBMCs were thawed and rested overnight at 37 °C and 5% carbon dioxide in complete RPMI medium. After overnight rest, PBMCs were stimulated for 6 h with 2μg/mL of SARS-CoV-2 peptide pools, Influenza, HIV-1 Gag or cytomegalovirus (CMV)-pp65 peptide pools, or with 0.005% dimethyl sulphoxide (DMSO) as a negative control in the presence of αCD28/αCD49d co-Stim antibodies (1 μg ml^{-1}) GolgiStop (containing Monensin, 2 μmol/L), GolgiPlug (containing brefeldin A, 10 μg ml^{-1}) (BD Biosciences) and anti-CD107α BV421 antibody (BD Biosciences). After stimulation, cells were washed and stained with anti-CCR7 (BioLegend) for 30 min at 37 °C and then surface stained at 4°C for 20 min with different combinations of surface antibodies in the presence of fixable live/dead stain (Invitrogen). Cells were then fixed and permeabilised (CytoFix/CytoPerm; BD Biosciences) followed by intracellular cytokine with IFN-γ APC, CD154 PE-Cy7 (BioLegend), TNF-α FITC (BD Biosciences) and PerCP-eFluor 710 IL-2 (eBioscience). Samples were acquired on a BD Fortessa X20 using BD FACSDiva8.0 (BD Bioscience) and data analysed using FlowJo 10 (TreeStar). The gates applied for the identification of virus-specific CD4 and CD8 T cells were based on the double-positive populations for interferon-γ (IFN-γ), Tumour necrosis factor (TNF-α), interleukin-2 (IL-2), and CD40 ligand (CD154). The total population of SARS-CoV-2 CD4 T cells was calculated by summing the magnitude of $CD154^{+}IFN\text{-}\gamma^{+}$, $CD154^{+}IL\text{-}2^{+}$, and $CD154^{+}$ $TNF\text{-}\alpha^{+}$ responses; SARS-CoV-2 CD8 T cells were defined as ($IFN\text{-}\gamma^{+}TNF\text{-}\alpha^{+}$, $IFN\text{-}\gamma^{+}IL\text{-}2^{+}$). Antibodies used in the ICS assay are listed in **Table S2**.

Statistics:

Prism 8 (GraphPad Software) was used for statistical analysis as follows: the Mann–Whitney *U*-test was used for single comparisons of independent groups, the Wilcoxon-test paired *t*-test was used to compare two paired groups. The non-parametric Spearman test was used for correlation analysis. The statistical significances are indicated in the figures (*$p < 0.05$, **$p < 0.01$, ***$p < 0.001$, and ****$p < 0.0001$). Polyfunctionality tests were performed in SPICE version 6.0.

Acknowledgments: We are grateful to Rebecca Matthews, Thomas Fernandez, Nnenna Ngwu the clinical research teams at Mortimer Market Centre and Ian Charleson Day Centre and all the clinic staff and participants. We would like to thank Chloe Rees-Spear for technical assistance and James E. Voss for the kind gift of HeLa cells stably expressing ACE2.

Funding: This work was supported by MRC grant MR/M008614 and NIH R01AI55182 (DP) and by UCL Coronavirus Response Fund (LEM) made possible through generous donations from UCL's supporters, alumni and friends**.** LEM is supported by a Medical Research Council Career Development Award (MR/R008698/1). ET is supported by a Medical Research Council DTP studentship (MR/N013867/1). DHB is supported by a Wellcome Trust PhD studentship in the Genomics and Statistical medicine doctoral training programme in Oxford.

Author contributions: AA, EGM, ET performed experiments, acquisition of data, analysis and drafting of the manuscript; DHB, JK, BC, NFP, LM, AR, CR, CE performed experiments and contributed to acquisition of data and analysis; PC, PP, LW, FB, SK, TD, LD, SRJ contributed to study design, data interpretation and critical editing of the manuscript. LEM, DP: conception and design of study, data analysis and interpretation, critical revision of the manuscript and study supervision.

687

688 **Competing interests:** The authors have declared that no conflict of interest exists.

689 **Data and materials availability**: Data can be made available by request to the corresponding
690 authors.

691

692 **Figure Legends:**

693 **Fig. 1**. **Antibody response in HIV positive and negative donors recovered from COVID-19**
694 **disease. (A)** Seropositivity screen of plasma samples for antibodies against the external Spike
695 antigen, using a recombinant Spike $S1_{1\text{-}530}$ subunit protein (S1), and against the full-length
696 internal Nucleoprotein (N) antigen to confirm prior infection in HIV negative and positive
697 donors. A sample absorbance greater than 4-fold above the average background of the assay was
698 regarded as positive. Black dots denote laboratory confirmed cases and grey dots
699 suspected/household contacts. **(B)** Comparison of S1 IgG and N IgG antibody titers in HIV
700 negative and **(C)** HIV positive donors. Red dots: hospitalized cases; Black dots: mild (non-
701 hospitalized cases); blue dots: asymptomatic cases. **(D)** Correlation between S1 IgG and N IgG
702 titers in HIV negative and positive donors. **(E)** Neutralization titers in HIV negative and positive
703 donors. Dotted lines indicate detection limit, minimum ID50 and potent levels >1000. **(F)**
704 Proportion of HIV negative and positive donors with neutralizing antibodies within the given
705 ranges. **(G)** Correlation between S1 IgG titers and neutralization titers in HIV negative and
706 positive donors. The non-parametric Spearman test was used for correlation analysis. *$p < 0.05$,
707 **$p<0.01$

708

Fig. 2. Similar SARS-CoV-2 specific T cell responses by IFN-γ-ELISpot in HIV positive and negative donors. (**A**) Genome organization of SARS-CoV-2 (**B**) Dominance of the IFN-γ-ELISpot responses. Heatmap depicting the magnitude of the IFN-γ-ELISpot responses to the different SARS-CoV-2 peptide pools in HIV negative and HIV positive individuals. (n=30 in each group) (**C**) Magnitude of the IFN-γ-ELISpot responses. IFN-γ SFU/10^6 PBMCs are shown for SARS-CoV-2 Spike (S), Membrane (M) and Nucleocapsid (N) between HIV negative (green) and HIV positive (red). (n=30 per group). (**D**) Magnitude of the IFN-γ-ELISpot responses for Total SARS-CoV-2 responses (S, M, N, ORF3a, ORF6, ORF7, ORF8 and Env), FEC and HIV Gag between HIV negative (green) and HIV positive (red). (n=30 per group). (**E**) Hierarchy of the IFNγ-ELISpot responses. IFN-γ SFU/10^6 PBMCs responses in order of magnitude within each group with the contribution of the responses to a specific pool shown by color legend. (**F**) Diversity of the IFN-γ-ELISpot responses. Number of pools each of the donors has shown positive responses in the IFN-γ-ELISpot assay. The total of SARS-CoV-2 pools tested was 7. (**G**) Proportion of T cell response magnitude in the HIV negative and HIV positive individuals. (**H**) Correlation between CD4:CD8 ratio in HIV infected individuals with their total SARS-CoV-2 responses, depicting disease severity per each donor (Red dots: hospitalized cases; Black dots: non-hospitalized cases; blue dots: asymptomatic cases.). The non-parametric Spearman test was used for correlation analysis. Two-way ANOVA was used for groups comparison. *$p < 0.05$, **$p<0.01$.

Fig. 3. Interrelations between T cell and antibody responses in HIV positive and negative donors. (A) Correlation of total SARS-CoV-2 responses with S1 IgG titers in HIV negative and (**B**) HIV positive. (**C**) Correlation of total SARS-CoV-2 responses with N IgG titers in HIV

732 negative and (**D**) HIV positive subjects. Red dots: hospitalized cases; Black dots: non-
733 hospitalized cases. **(E)** Hierarchy of the T cell responses ordered by the neutralizing capacity by
734 their antibody titers for HIV negative and (**F**) HIV positive donors. The non-parametric
735 Spearman test was used for correlation analysis. *p < 0.05, **p<0.01
736
737 **Fig. 4. Composition of SARS-CoV-2-specific T cells in convalescent HIV negative and HIV**
738 **positive individuals.** Intracellular cytokine staining (ICS) was performed to detect cytokine-
739 producing T cells to the indicated peptide pools in HIV negative (HIV-, n=12) and HIV positive
740 individuals (HIV+, n=11). **(A)** Representative flow cytometric plots for the identification of
741 antigen-specific CD4 T cells based on double expressions ($CD154^+IFN\text{-}\gamma^+$, $CD154^+IL\text{-}2^+$, and
742 $CD154^+TNF\text{-}\alpha^+$) following 6-hour stimulation media alone (control) or overlapping SARS-CoV-
743 2 peptides against Spike pool 1 and 2 (Spike), nucleoprotein (N), and membrane protein (M)
744 directly *ex vivo*. **(B)** Frequency of aggregated CD4 T cell responses ($CD154^+IFN\text{-}\gamma^+$, $CD154^+IL\text{-}$
745 2^+, and $CD154^+TNF\text{-}\alpha^+$) against Spike, M/N or combined (Spike and M/N) peptide pools. **(C)**
746 Pie charts representing the relative proportions of Spike, M/N, or total (combined Spike and
747 M/N) CD4 T cell responses for one (grey), two (green) or three (dark blue) cytokines, and pie
748 arcs denoting IFN-γ, TNF-α and IL-2. **(D)** Representative flow cytometric plots for the
749 identification of antigen-specific CD8 T cells based on the expression of ($IFN\text{-}\gamma^+$, $TNF\text{-}\alpha^+$, and
750 $IL\text{-}2^+$) against the specified peptide pools or media alone (control). **(E)** Proportion of aggregated
751 CD8 T cell responses against Spike, M/N or combined (Spike and M/N) responses. **(F)** Pie charts
752 representing the relative proportions of Spike, M/N and combined CD8 T cell responses for one
753 (grey), two (green) or three (dark blue) cytokines, and pie arcs showing IFN-γ, TNF-α and IL-2.
754 (**G)** Comparison of the frequencies of summed SARS-CoV-2-specific CD4 and CD8 T cell

responses against Spike and M/N proteins. **(H)** Correlation between the frequency of total SARS-CoV-2 specific-CD4 T cells and overall T cell responses detected by IFN-γ ELISpot responses or **(I)** ID50 neutralization titer (log10) in HIV negative and HIV positive individuals. Error bars represent SEM. The non-parametric Spearman test was used for correlation analysis; p values for individual correlation analysis within groups, HIV- (green) or HIV+(red) or combined correlation analysis (black) are presented. Significance determined by Mann-Whitney *U* test or Wilcoxon matched- pairs signed rank test, *p<0.05, **p<0.01, ***p < 0.001. SPICE (simplified presentation of incredibly complex evaluations) was used for polyfunctional analysis.

Fig. 5. Phenotypic characterization of SARS-CoV-2-specific CD4 and CD8 T cells from convalescent HIV negative and HIV positive subjects. (A) Representative flow plots and **(B)** pie charts representing proportion of antigen-specific CD4 T cell with a $CD45RA^-/CCR7^+$ central memory (CM), $CD45RA^+/CCR7^+$ naïve, $CD45RA^+/CCR7^-$ terminally differentiated effector memory (TEMRA) and $CD45RA^-/CCR7^-$ effector memory (EM) phenotype from HIV negative (HIV-, n=12) and HIV positive individuals (HIV+, n=11) against SARS-CoV-2 Spike, M, N, CMV pp65 and HIV gag. **(C)** Representative flow plots and **(D)** pie charts representing proportion of $CD45RA^-/CCR7^+$ central memory (CM), $CD45RA^+/CCR7^+$ naïve, $CD45RA^+/CCR7^-$ terminally differentiated effector memory (TEMRA) and $CD45RA^-/CCR7^-$ effector memory (EM) antigen-specific CD8 T cell subsets against SARS-CoV-2 Spike, M, N, CMV pp65 and HIV gag. **(E)** Representative flow plots from an HIV negative donor (HIV-) and an HIV positive donor (HIV+) showing expression of CD154 and IFN-γ production from PD1+ and PD1- SARS-CoV-2-specific CD4 T cells and **(E)** paired analysis of responses in HIV negative (HIV-, n=12) and HIV positive (HIV+, n=11) individuals. **(F)** Correlation between

778 frequency of (PD-1^{+}CD154^{+}IFN-γ^{+} SARS-CoV-2-specific CD4 T cells and DPSO in both
779 groups. Significance determined by Wilcoxon matched-pairs signed rank test, *p<0.05,
780 **p<0.01, ***p < 0.001. The non-parametric Spearman test was used for correlation analysis; p
781 values for individual correlation analysis within groups, HIV-, HIV+, or combined correlation
782 analysis (black) are presented.
783
784 **Fig. 6. Immune profile relationships between convalescent HIV positive and negative**
785 **individuals. (A)** viSNE analysis of CD3 T cells in HIV negative (top panel) and HIV positive
786 donors (lower panel). Each point on the high-dimensional mapping represents an individual cell
787 and colour intensity represents expression of selected markers. (**B**) Frequency of CD4 and CD8 T
788 cells out of total lymphocytes in SARS-CoV-2 convalescent HIV negative (HIV-, n=26) and HIV
789 positive individuals (HIV+, n=19) via traditional gating. **(C)** Summary data of the proportion of
790 CD45RA^{-}/CCR7^{+} central memory (CM), CD45RA^{+}/CCR7^{+} naïve, CD45RA^{+}/CCR7^{-} terminally
791 differentiated effector memory (TEMRA) and CD45RA^{-}/CCR7^{-} effector memory (EM) CD4 and
792 CD8 T cell subsets it the study groups. **(D)** Correlation between CD4:CD8 ratio and frequency of
793 naïve CD4 T cells in HIV-positive individuals. **(E)** Correlation between frequency of naïve CD4
794 T cells and total SARS-CoV-2 T cell responses, detected via ELISpot, in HIV positive
795 individuals. **(F)** Correlation between frequency of naïve CD4 T cells and (**G**) naïve CD8 T cells
796 and age in HIV negative individuals. (**H**) Correlation between frequency of naïve CD4 T cells
797 and (**I**) naïve CD8 T cells age in HIV positive donors. Significance determined by Mann-
798 Whitney test, *p<0.05, **p<0.01, ***p < 0.001. The non-parametric Spearman test was used for
799 correlation analysis.

Supplementary Materials:

Fig. S1. Antigen binding screen and associations between humoral responses and cohort parameters. (A) Antigen binding screen in pre-pandemic samples from n=16 HIV positive donors and **(B)** the whole cohort with convalescent COVID-19 disease. Dotted lines indicate negative, low positive and positive threshold for absorbance [450nm]. **(C)** Correlation between age and S1 IgG titer according to gender in HIV negative donors and HIV positive subjects. **(D)** Correlation between age and ID50 according to gender in HIV negative donors and HIV positive subjects and **(E)** between DPSO and ID50 in the two study groups. **(F)** S1 IgG titer and ID50 levels summary dot plots according to ethnicity in HIV positive and negative donors. The non-parametric Spearman test was used for correlation analysis. *$p < 0.05$

Fig. S2. Magnitude of T cell responses and associations with HIV parameters, age, gender and ethnicity. (**A**) Percentage of responders to each peptide pools (**B**) Magnitude of the INF-γ-ELISpot responses. IFN-γ SFU/10^6 PBMCs are shown for SARS-CoV-2 ORF3a, ORF6, ORF7, ORF8 and Env between HIV negative (green) and HIV positive (red). (n=30 per group). (**C**) Magnitude of the total SARS-CoV-2 responses analyzed in pre-pandemic samples, confirmed SARS-CoV-2 and suspected cases with clinical definition but found to be SARS-CoV-2 seronegative on screening. In suspected cases, orange dots depict HIV negative and brown dots HIV positive donors. Correlation between CD4:CD8 ratio in HIV infected individuals with their (**D**) Nucleocapsid and (**E**) Membrane responses, depicting disease severity per donor. Correlation of total SARS-CoV-2 responses with age in (**F**) HIV negative and (**G**) HIV positive, depicting disease severity per donor. **(H)** Correlation of total SARS-CoV-2 responses with DPSO in HIV negative and (**J**) HIV positive, depicting disease severity per donor. (**J**) Magnitude of the total SARS-CoV-2 responses by ethnicity and **(K)** gender between HIV negative and HIV positive. The non-parametric Spearman test was used for correlation analysis. Two-way ANOVA was used for group comparison. *p < 0.05, **p<0.01.

Fig. S3. Cytokine profile of SARS-CoV-2-, CMV- and Gag- specific T cells

(A) Frequency of SARS-CoV-2-specific $CD154^+$ CD4 T cells identified by expression of IFN-γ^+, IL-2^+, or TNF-α^+ or overall responses with at least one of the three cytokines (IFN-γ, TNF- α and IL-2) against Spike (S1 and S2 pools) **(B)** M/N or **(C)** combined (Spike and M/N) responses in HIV-negative (HIV-, n=12) and HIV positive individuals (HIV+, n=11) recovering from COVID-19 disease. **(D)** Representative flow plots and summary data **(E)** showing frequencies of overall ($CD154^+$IFN-γ^+, $CD154^+$IL-2^+, or $CD154^+$TNF-α^+) SARS-CoV-2-, CMV-, or Gag-specific CD4

T cell responses in the study groups. **(F)** Frequency of SARS-CoV-2-specific CD8 T cells identified by expression of IFN-γ^+, IL-2^+ or TNF-α^+, or overall responses with at least one of the three cytokines (IFN-γ, TNF- α and IL-2) against Spike (S1 and S2 pools) **(G)** M/N **(H)** or combined (Spike and M/N) responses in HIV-negative (HIV-, n=12) and HIV-seropositive individuals (HIV+, n=11). **(I)** Representative flow plots and **(J)** summary data showing frequencies of overall (IFN-γ^+, IL-2^+, or TNF-α^+) SARS-CoV-2-, CMV-, or Gag-specific CD8 T cell responses in the study groups. Error bars represent SEM. The non-parametric Spearman test was used for correlation analysis; p values for individual correlation analysis within groups, HIV- (green) or HIV+ (red) or combined correlation analysis (black) are presented. Significance determined by Mann-Whitney *U* test or Wilcoxon matched- pairs signed rank test, *p<0.05, **p<0.01, ***p < 0.001.

Fig. S4. Association between T cell immunophenotyping and SARS-CoV-2 adaptive immune responses

(A) Representative flow plots and **(B)** summary data of the frequency of $CD38^+$ $HLADR^+$ CD4 and CD8 T cells, and correlations between percentage of $CD38^+$ $HLADR^+$ CD4 and CD8 T cells and total SARS-CoV-2-specific T cell responses in HIV-seronegative (HIV-, n=26) and HIV positive individuals (HIV+, n=19). **(C)** Representative flow plots and **(D)** summary data of frequency of PD-1^+ $TIGIT^+$ CD4 and CD8 T cells, and correlations between percentage of PD-1^+ $TIGIT^+$ CD4 and CD8 T cells and total SARS-CoV-2-specific T cell responses. **(E)** Representative flow plots showing the gating strategy used to define total circulating and activated Tfh subsets in the study groups and summary data. **(F)** Correlations between percentage of activated Tfh and S1 IgG or N IgG titers. Significance determined by Mann-

Whitney test, *p<0.05, **p<0.01, ***p < 0.001. The non-parametric Spearman test was used for correlation analysis; combined correlation analysis is depicted.

References:

Altmann, D. M. and Boyton, R. J. (2020), 'SARS-CoV-2 T cell immunity: Specificity, function, durability, and role in protection', *Sci Immunol,* 5 (49).

Amir el, A. D., et al. (2013), 'viSNE enables visualization of high dimensional single-cell data and reveals phenotypic heterogeneity of leukemia', *Nat Biotechnol,* 31 (6), 545-52.

Anderson, E. J., et al. (2020), 'Safety and Immunogenicity of SARS-CoV-2 mRNA-1273 Vaccine in Older Adults', *N Engl J Med*, 383 (25), 2427-38.

Annika Fendler, Lewis Au, Laura Amanda Boos, Fiona Byrne, Scott T.C. Shepherd, Ben Shum, Camille L. Gerard, Barry Ward, Wenyi Xie, Maddalena Cerrone, Georgina H. Cornish, Martin Pule, Leila Mekkaoui, Kevin W. Ng, Richard Stone, Camila Gomes, Helen R. Flynn, Ana Agua-Doce, Phillip Hobson, Simon Caidan, Mike Howell, Robert Goldstone, Mike Gavrielides, Emma Nye, Bram Snijders, James Macrae, Jerome Nicod, Adrian Hayday, Firza Gronthoud, Christina Messiou, David Cunningham, Ian Chau, Naureen Starling, Nicholas Turner, Jennifer Rusby, Liam Welsh, Nicholas van As, Robin Jones, Joanne Droney, Susana Banerjee, Kate Tatham, Shaman Jhanji, Mary O'Brien, Olivia Curtis, Kevin Harrington, Shreerang Bhide, Tim Slattery, Yasir Khan, Zayd Tippu, Isla Leslie, Spyridon Gennatas, Alicia Okines, Alison Reid, Kate Young, Andrew Furness, Lisa Pickering, Sonia Ghandi, Steve Gamblin, Charles Swanton, Emma Nicholson, Sacheen Kumar, Nadia Yousaf, Katalin Wilkinson, Anthony Swerdlow, Ruth Harvey,

George Kassiotis, Robert Wilkinson, James Larkin, Samra Turajlic (2020), 'Adaptive immunity to SARS-CoV-2 in cancer patients: The CAPTURE study', *medRxiv 2020.12.21.20248608*.

Appay, V. and Sauce, D. (2008), 'Immune activation and inflammation in HIV-1 infection: causes and consequences', *J Pathol*, 214 (2), 231-41.

Bhaskaran, K., et al. (2021), 'HIV infection and COVID-19 death: a population-based cohort analysis of UK primary care data and linked national death registrations within the OpenSAFELY platform', *Lancet HIV*, 8 (1), e24-e32.

Blanco, J. L., et al. (2020), 'COVID-19 in patients with HIV: clinical case series', *Lancet HIV*, 7 (5), e314-e16.

Boppana, S., et al. (2020), 'SARS-CoV-2-specific peripheral T follicular helper cells correlate with neutralizing antibodies and increase during convalescence', *medRxiv*.

Boulle, A., et al. (2020), 'Risk factors for COVID-19 death in a population cohort study from the Western Cape Province, South Africa', *Clin Infect Dis.*

Braun, J., et al. (2020), 'SARS-CoV-2-reactive T cells in healthy donors and patients with COVID-19', *Nature*, 587 (7833), 270-74.

Breton, G., et al. (2020), 'Persistent Cellular Immunity to SARS-CoV-2 Infection', *bioRxiv*.

Breton, G., et al. (2013), 'Programmed death-1 is a marker for abnormal distribution of naive/memory T cell subsets in HIV-1 infection', *J Immunol*, 191 (5), 2194-204.

C Rees-Spear, L Muir, SA Griffith, J Heaney, Y Aldon, JL Snitselaar, P Thomas, C Graham, J Seow, N Lee, A Rosa, C Roustan, CF Houlihan, RW Sanders, R Gupta, P Cherepanov, H Stauss, E Nastouli, KJ Doores, MJ van Gils, LE McCoy (2021), 'The impact of Spike mutations on SARS-CoV-2 neutralization', *bioRxiv*.

914 Calvet, J., et al. (2020), 'CD4 and CD8 Lymphocyte Counts as Surrogate Early Markers for
915 Progression in SARS-CoV-2 Pneumonia: A Prospective Study', *Viruses*, 12 (11).
916 Chen, Z. and John Wherry, E. (2020), 'T cell responses in patients with COVID-19', *Nat Rev*
917 *Immunol*, 20 (9), 529-36.
918 Cooper, T. J., et al. (2020), 'Coronavirus disease 2019 (COVID-19) outcomes in HIV/AIDS
919 patients: a systematic review', *HIV Med*, 21 (9), 567-77.
920 Crotty, S. (2015), 'A brief history of T cell help to B cells', *Nat Rev Immunol*, 15 (3), 185-9.
921 Dan, J. M., et al. (2020), 'Immunological memory to SARS-CoV-2 assessed for up to eight
922 months after infection', *bioRxiv*.
923 De Biasi, S., et al. (2020), 'Marked T cell activation, senescence, exhaustion and skewing
924 towards TH17 in patients with COVID-19 pneumonia', *Nat Commun*, 11 (1), 3434.
925 De Francesco, D., et al. (2019), 'Do people living with HIV experience greater age advancement
926 than their HIV-negative counterparts?', *AIDS*, 33 (2), 259-68.
927 Deeks, S. G. and Phillips, A. N. (2009), 'HIV infection, antiretroviral treatment, ageing, and non-
928 AIDS related morbidity', *BMJ*, 338, a3172.
929 Douek, D. C., et al. (1998), 'Changes in thymic function with age and during the treatment of
930 HIV infection', *Nature*, 396 (6712), 690-5.
931 El-Far, M., et al. (2008), 'T-cell exhaustion in HIV infection', *Curr HIV/AIDS Rep*, 5 (1), 13-9.
932 Folegatti, P. M., et al. (2020), 'Safety and immunogenicity of the ChAdOx1 nCoV-19 vaccine
933 against SARS-CoV-2: a preliminary report of a phase 1/2, single-blind, randomised
934 controlled trial', *Lancet*, 396 (10249), 467-78.
935 Gaebler, C., et al. (2020), 'Evolution of Antibody Immunity to SARS-CoV-2', *bioRxiv*.

George, V. K., et al. (2015), 'HIV infection Worsens Age-Associated Defects in Antibody Responses to Influenza Vaccine', *J Infect Dis*, 211 (12), 1959-68.

Geretti, A. M., et al. (2020), 'Outcomes of COVID-19 related hospitalization among people with HIV in the ISARIC WHO Clinical Characterization Protocol (UK): a prospective observational study', *Clin Infect Dis*.

Grifoni, A., et al. (2020), 'Targets of T Cell Responses to SARS-CoV-2 Coronavirus in Humans with COVID-19 Disease and Unexposed Individuals', *Cell*, 181 (7), 1489-501 e15.

Guan, W. J., et al. (2020), 'Clinical Characteristics of Coronavirus Disease 2019 in China', *N Engl J Med*, 382 (18), 1708-20.

Guaraldi, G., et al. (2011), 'Premature age-related comorbidities among HIV-infected persons compared with the general population', *Clin Infect Dis*, 53 (11), 1120-6.

Gupta, R. K., et al. (2019), 'HIV-1 remission following CCR5Delta32/Delta32 haematopoietic stem-cell transplantation', *Nature*, 568 (7751), 244-48.

Harris, T. G., Rabkin, M., and El-Sadr, W. M. (2018), 'Achieving the fourth 90: healthy aging for people living with HIV', *AIDS*, 32 (12), 1563-69.

Helleberg, M., et al. (2015), 'Course and Clinical Significance of CD8+ T-Cell Counts in a Large Cohort of HIV-Infected Individuals', *J Infect Dis*, 211 (11), 1726-34.

Hoffmann, C., et al. (2020), 'Immune deficiency is a risk factor for severe COVID-19 in people living with HIV', *HIV Med*.

Houriiyah Tegally, Eduan Wilkinson, Marta Giovanetti, Arash Iranzadeh, Vagner Fonseca, Jennifer Giandhari, Deelan Doolabh, Sureshnee Pillay, Emmanuel James San, Nokukhanya Msomi, Koleka Mlisana, Anne von Gottberg, Sibongile Walaza, Mushal Allam, Arshad Ismail, Thabo Mohale, Allison J Glass, Susan Engelbrecht, Gert Van Zyl,

959 Wolfgang Preiser, Francesco Petruccione, Alex Sigal, Diana Hardie, Gert Marais, Marvin
960 Hsiao, Stephen Korsman, Mary-Ann Davies, Lynn Tyers, Innocent Mudau, Denis York,
961 Caroline Maslo, Dominique Goedhals, Shareef Abrahams, Oluwakemi Laguda-Akingba,
962 Arghavan Alisoltani-Dehkordi, Adam Godzik, Constantinos Kurt Wibmer, Bryan Trevor
963 Sewell, José Lourenço, Luiz Carlos Junior Alcantara, Sergei L Kosakovsky Pond, Steven
964 Weaver, Darren Martin, Richard J Lessells, Jinal N Bhiman, Carolyn Williamson, Tulio
965 de Oliveira (2020), 'Emergence and rapid spread of a new severe acute respiratory
966 syndrome-related coronavirus 2 (SARS-CoV-2) lineage with multiple spike mutations in
967 South Africa', *medRxiv 2020.12.21.20248640*.

968 Inciarte, A., et al. (2020), 'Clinical characteristics, risk factors, and incidence of symptomatic
969 coronavirus disease 2019 in a large cohort of adults living with HIV: a single-center,
970 prospective observational study', *AIDS*, 34 (12), 1775-80.

971 Juno, J. A., et al. (2020), 'Humoral and circulating follicular helper T cell responses in recovered
972 patients with COVID-19', *Nat Med*, 26 (9), 1428-34.

973 Kim, D. S., Rowland-Jones, S., and Gea-Mallorqui, E. (2020), 'Will SARS-CoV-2 Infection
974 Elicit Long-Lasting Protective or Sterilising Immunity? Implications for Vaccine
975 Strategies (2020)', *Front Immunol*, 11, 571481.

976 Laidlaw, B. J., Craft, J. E., and Kaech, S. M. (2016), 'The multifaceted role of CD4(+) T cells in
977 CD8(+) T cell memory', *Nat Rev Immunol*, 16 (2), 102-11.

978 Le Bert, N., et al. (2020), 'SARS-CoV-2-specific T cell immunity in cases of COVID-19 and
979 SARS, and uninfected controls', *Nature*, 584 (7821), 457-62.

980 Lumley, S. F., et al. (2020), 'Antibody Status and Incidence of SARS-CoV-2 Infection in Health
981 Care Workers', *N Engl J Med*.

Mathew, D., et al. (2020), 'Deep immune profiling of COVID-19 patients reveals distinct immunotypes with therapeutic implications', *Science*, 369 (6508).

Moir, S. and Fauci, A. S. (2017), 'B-cell responses to HIV infection', *Immunol Rev*, 275 (1), 33-48.

Ng, K. W., et al. (2020), 'Preexisting and de novo humoral immunity to SARS-CoV-2 in humans', *Science*, 370 (6522), 1339-43.

O'Nions, J., et al. (2021), 'SARS-CoV-2 antibody responses in patients with acute leukaemia', *Leukemia*, 35 (1), 289-92.

Oja, A. E., et al. (2020), 'Divergent SARS-CoV-2-specific T- and B-cell responses in severe but not mild COVID-19 patients', *Eur J Immunol*, 50 (12), 1998-2012.

Opportunistic Infections Project Team of the Collaboration of Observational, H. I. V. Epidemiological Research in Europe in EuroCoord, et al. (2012), 'CD4 cell count and the risk of AIDS or death in HIV-Infected adults on combination antiretroviral therapy with a suppressed viral load: a longitudinal cohort study from COHERE', *PLoS Med*, 9 (3), e1001194.

Owen, R. E., et al. (2007), 'Loss of T cell responses following long-term cryopreservation', *J Immunol Methods*, 326 (1-2), 93-115.

Pallikkuth, S., et al. (2017), 'T Follicular Helper Cells and B Cell Dysfunction in Aging and HIV-1 Infection', *Front Immunol*, 8, 1380.

Pallikkuth, S., et al. (2012), 'Impaired peripheral blood T-follicular helper cell function in HIV-infected nonresponders to the 2009 H1N1/09 vaccine', *Blood*, 120 (5), 985-93.

1003 Peng, Y., et al. (2020), 'Broad and strong memory CD4(+) and CD8(+) T cells induced by
1004 SARS-CoV-2 in UK convalescent individuals following COVID-19', *Nat Immunol,* 21
1005 (11), 1336-45.
1006 Pickering, S., et al. (2020), 'Comparative assessment of multiple COVID-19 serological
1007 technologies supports continued evaluation of point-of-care lateral flow assays in hospital
1008 and community healthcare settings', *PLoS Pathog,* 16 (9), e1008817.
1009 Polack, F. P., et al. (2020), 'Safety and Efficacy of the BNT162b2 mRNA Covid-19 Vaccine', *N*
1010 *Engl J Med,* 383 (27), 2603-15.
1011 Reynolds, C. J., et al. (2020), 'Discordant neutralizing antibody and T cell responses in
1012 asymptomatic and mild SARS-CoV-2 infection', *Sci Immunol,* 5 (54).
1013 Rha, M. S., et al. (2021), 'PD-1-Expressing SARS-CoV-2-Specific CD8(+) T Cells Are Not
1014 Exhausted, but Functional in Patients with COVID-19', *Immunity,* 54 (1), 44-52 e3.
1015 Ripperger, T. J., et al. (2020), 'Orthogonal SARS-CoV-2 Serological Assays Enable Surveillance
1016 of Low-Prevalence Communities and Reveal Durable Humoral Immunity', *Immunity,* 53
1017 (5), 925-33 e4.
1018 Robbiani, D. F., et al. (2020), 'Convergent antibody responses to SARS-CoV-2 in convalescent
1019 individuals', *Nature,* 584 (7821), 437-42.
1020 Rodda, L. B., et al. (2021), 'Functional SARS-CoV-2-Specific Immune Memory Persists after
1021 Mild COVID-19', *Cell,* 184 (1), 169-83 e17.
1022 Roederer, M., et al. (1995), 'CD8 naive T cell counts decrease progressively in HIV-infected
1023 adults', *J Clin Invest,* 95 (5), 2061-6.

1024 Rydyznski Moderbacher, C., et al. (2020), 'Antigen-Specific Adaptive Immunity to SARS-CoV-
1025 2 in Acute COVID-19 and Associations with Age and Disease Severity', *Cell*, 183 (4),
1026 996-1012 e19.

1027 SA Kemp, DA Collier, R Datir, S Gayed, A Jahun, M Hosmillo, IATM Ferreira, C Rees-Spear, P
1028 Mlcochova, Ines Ushiro Lumb, David Roberts, Anita Chandra, N Temperton, The
1029 CITIID-NIHR BioResource COVID-19 Collaboration, The COVID-19 Genomics UK
1030 (COG-UK) Consortium, K Sharrocks, E Blane, JAG Briggs, MJ van Gils, KGC Smith,
1031 JR Bradley, C Smith, RA Goldstein, IG Goodfellow, A Smielewska, JP Skittrall, T
1032 Gouliouris, E Gkrania-Klotsas, CJR Illingworth, LE McCoy, RK Gupta (2020),
1033 'Neutralising antibodies drive Spike mediated SARS-CoV-2 evasion', *medRxiv*
1034 *2020.12.05.20241927*.

1035 Sandile Cele, Inbal Gazy, Laurelle Jackson, Shi-Hsia Hwa, Houriiyah Tegally, Gila Lustig,
1036 Jennifer Giandhari, Sureshnee Pillay, Eduan Wilkinson, Yeshnee Naidoo, Farina Karim,
1037 Yashica Ganga, Khadija Khan, Alejandro B. Balazs, Bernadett I. Gosnell, Willem
1038 Hanekom, Mahomed-Yunus S. Moosa, NGS-SA, COMMIT-KZN Team, Richard J.
1039 Lessells, Tulio de Oliveira, Alex Sigal (2021), 'Escape of SARS-CoV-2 501Y.V2
1040 variants from neutralization by convalescent plasma', *medRxiv 2021.01.26.21250224*.

1041 Sattler, A., et al. (2020), 'SARS-CoV-2-specific T cell responses and correlations with COVID-
1042 19 patient predisposition', *J Clin Invest*, 130 (12), 6477-89.

1043 Sekine, T., et al. (2020), 'Robust T Cell Immunity in Convalescent Individuals with
1044 Asymptomatic or Mild COVID-19', *Cell*, 183 (1), 158-68 e14.

1045 Seow, J., et al. (2020), 'Longitudinal observation and decline of neutralizing antibody responses
1046 in the three months following SARS-CoV-2 infection in humans', *Nat Microbiol,* 5 (12),
1047 1598-607.
1048 Serrano-Villar, S., et al. (2014a), 'The CD4:CD8 ratio is associated with markers of age-
1049 associated disease in virally suppressed HIV-infected patients with immunological
1050 recovery', *HIV Med,* 15 (1), 40-9.
1051 Serrano-Villar, S., et al. (2014b), 'Increased risk of serious non-AIDS-related events in HIV-
1052 infected subjects on antiretroviral therapy associated with a low CD4/CD8 ratio', *PLoS*
1053 *One,* 9 (1), e85798.
1054 Serrano-Villar, S., et al. (2014c), 'HIV-infected individuals with low CD4/CD8 ratio despite
1055 effective antiretroviral therapy exhibit altered T cell subsets, heightened CD8+ T cell
1056 activation, and increased risk of non-AIDS morbidity and mortality', *PLoS Pathog,* 10
1057 (5), e1004078.
1058 Sigel, K., et al. (2020), 'Coronavirus 2019 and People Living With Human Immunodeficiency
1059 Virus: Outcomes for Hospitalized Patients in New York City', *Clin Infect Dis,* 71 (11),
1060 2933-38.
1061 Song, J. W., et al. (2020), 'Immunological and inflammatory profiles in mild and severe cases of
1062 COVID-19', *Nat Commun,* 11 (1), 3410.
1063 Tan, A. T., et al. (2021), 'Early induction of functional SARS-CoV-2-specific T cells associates
1064 with rapid viral clearance and mild disease in COVID-19 patients', *Cell Rep,* 34 (6),
1065 108728.

1066 Tang, F., et al. (2011), 'Lack of peripheral memory B cell responses in recovered patients with
1067 severe acute respiratory syndrome: a six-year follow-up study', *J Immunol*, 186 (12),
1068 7264-8.
1069 V Hall, S Foulkes, A Charlett, A Atti, EJM Monk, R Simmons, E Wellington, MJ Cole, A Saei,
1070 B Oguti, K Munro, S Wallace, PD Kirwan, M Shrotri, A Vusirikala, S Rokadiya, M Kall,
1071 M Zambon, M Ramsay, T Brooks, SIREN Study Group, CS Brown, MA Chand, S
1072 Hopkins (2020), 'Do antibody positive healthcare workers have lower SARS-CoV-2
1073 infection rates than antibody negative healthcare workers? Large multi-centre prospective
1074 cohort study (the SIREN study), England: June to November 2020', *medRxiv*
1075 *2021.01.13.21249642*.
1076 Wajnberg, A., et al. (2020), 'Robust neutralizing antibodies to SARS-CoV-2 infection persist for
1077 months', *Science*, 370 (6521), 1227-30.
1078 Wang, M., et al. (2020), 'One case of coronavirus disease 2019 (COVID-19) in a patient co-
1079 infected by HIV with a low CD4(+) T-cell count', *Int J Infect Dis*, 96, 148-50.
1080 Wibmer, C. K., et al. (2021), 'SARS-CoV-2 501Y.V2 escapes neutralization by South African
1081 COVID-19 donor plasma', *bioRxiv*.
1082 Williamson, E. J., et al. (2020), 'Factors associated with COVID-19-related death using
1083 OpenSAFELY', *Nature*, 584 (7821), 430-36.
1084 Wu, Z. and McGoogan, J. M. (2020), 'Characteristics of and Important Lessons From the
1085 Coronavirus Disease 2019 (COVID-19) Outbreak in China: Summary of a Report of
1086 72314 Cases From the Chinese Center for Disease Control and Prevention', *JAMA*, 323
1087 (13), 1239-42.

1088 Yu, J., et al. (2020), 'DNA vaccine protection against SARS-CoV-2 in rhesus macaques',
1089 *Science,* 369 (6505), 806-11.
1090 Zhang, J., et al. (2021), 'Spike-specific circulating T follicular helper cell and cross-neutralizing
1091 antibody responses in COVID-19-convalescent individuals', *Nat Microbiol,* 6 (1), 51-58.
1092 Zheng, M., et al. (2020), 'Functional exhaustion of antiviral lymphocytes in COVID-19 patients',
1093 *Cell Mol Immunol,* 17 (5), 533-35.
1094 Zhou, R., et al. (2020), 'Acute SARS-CoV-2 Infection Impairs Dendritic Cell and T Cell
1095 Responses', *Immunity,* 53 (4), 864-77 e5.
1096 Zimmerli, S. C., et al. (2005), 'HIV-1-specific IFN-gamma/IL-2-secreting CD8 T cells support
1097 CD4-independent proliferation of HIV-1-specific CD8 T cells', *Proc Natl Acad Sci U S*
1098 *A,* 102 (20), 7239-44.
1099 Zufferey, R., et al. (1997), 'Multiply attenuated lentiviral vector achieves efficient gene delivery
1100 in vivo', *Nat Biotechnol,* 15 (9), 871-5.
1101 Zuo J, Dowell A, Pearce H, et al. (2020), 'Robust SARS-CoV-2-specific T-cell immunity is
1102 maintained at 6 months following primary infection', *BioRxiv 2020.11.01.362319v1.*
1103

Figure 1

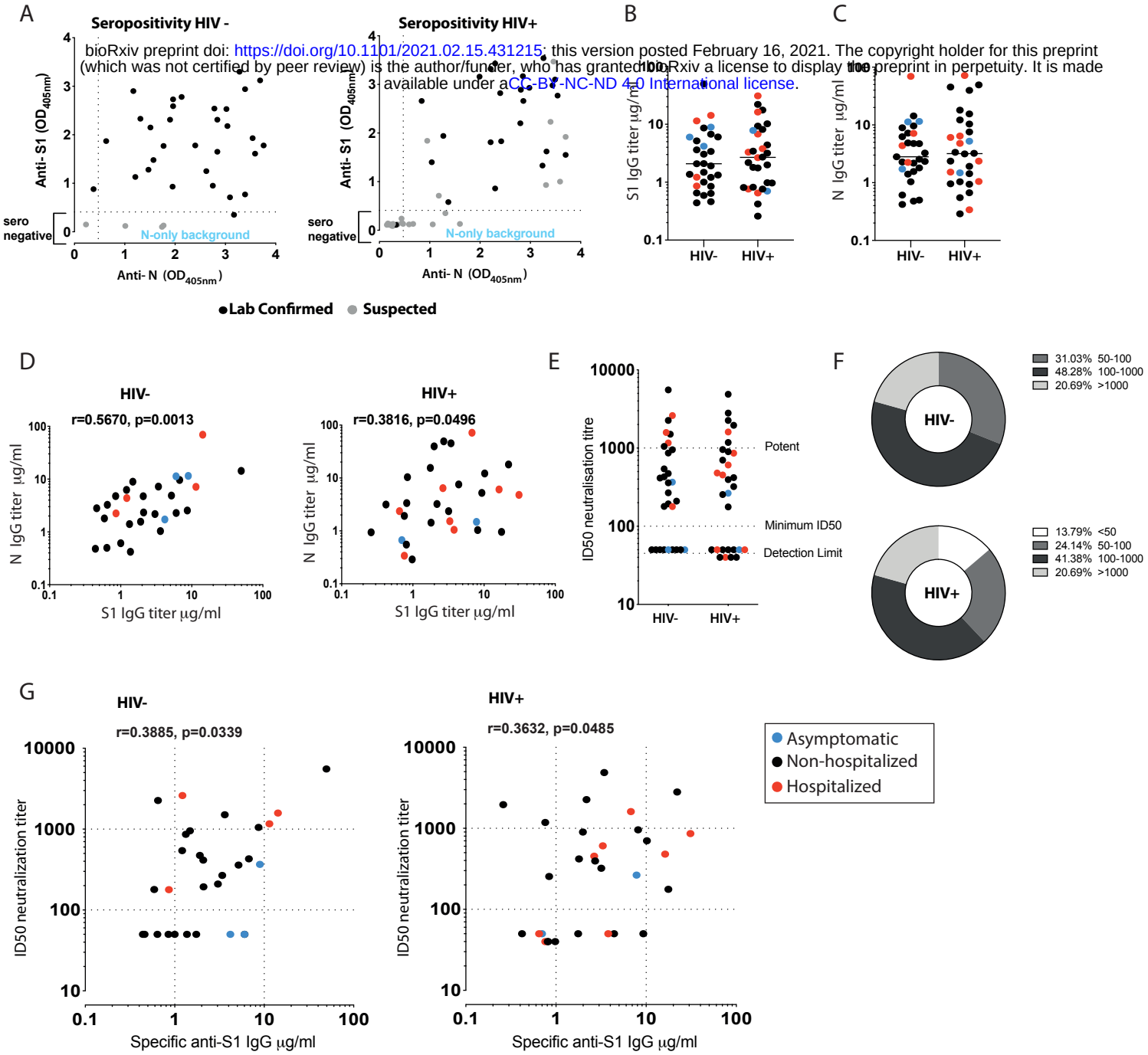

Figure 2

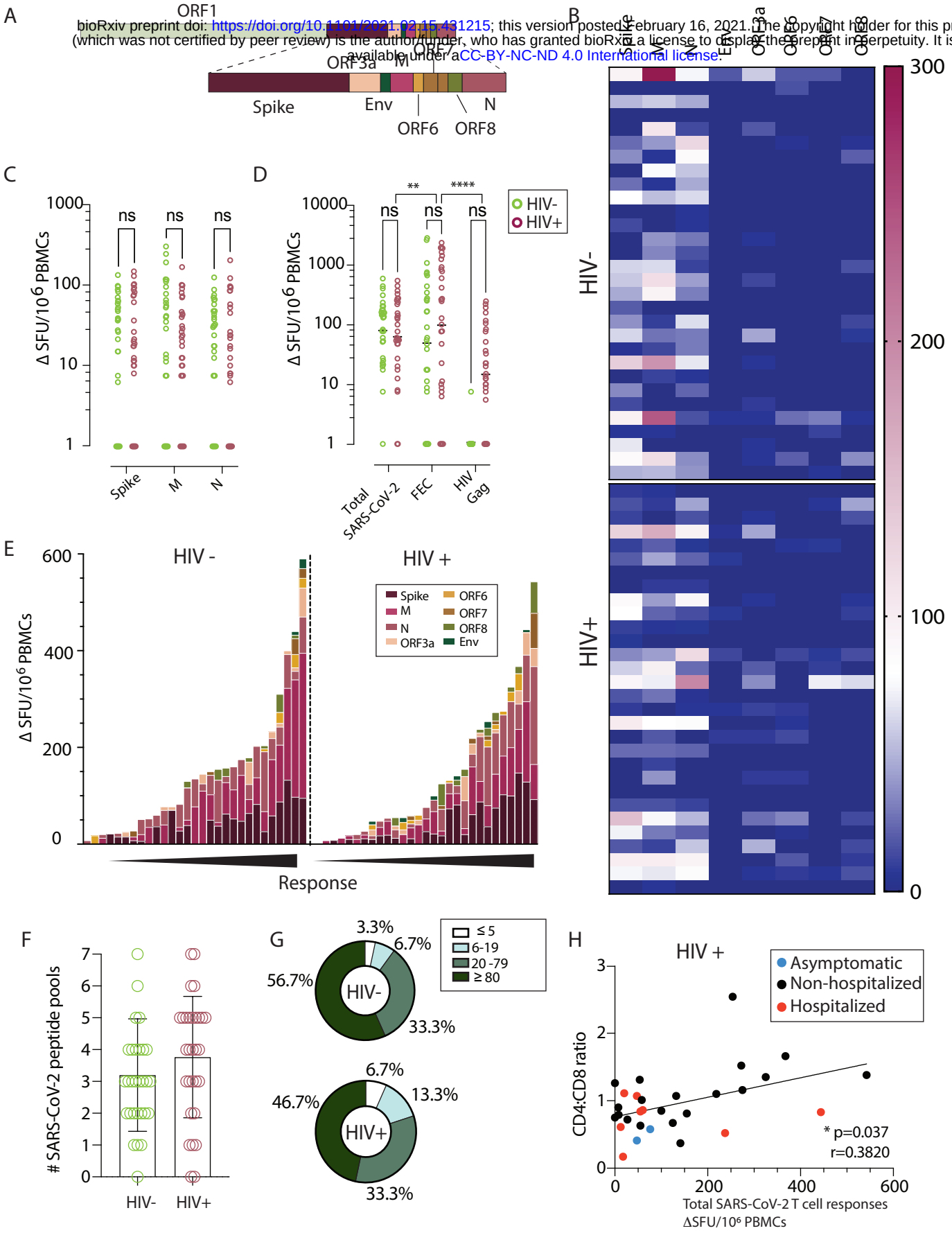

Figure 3

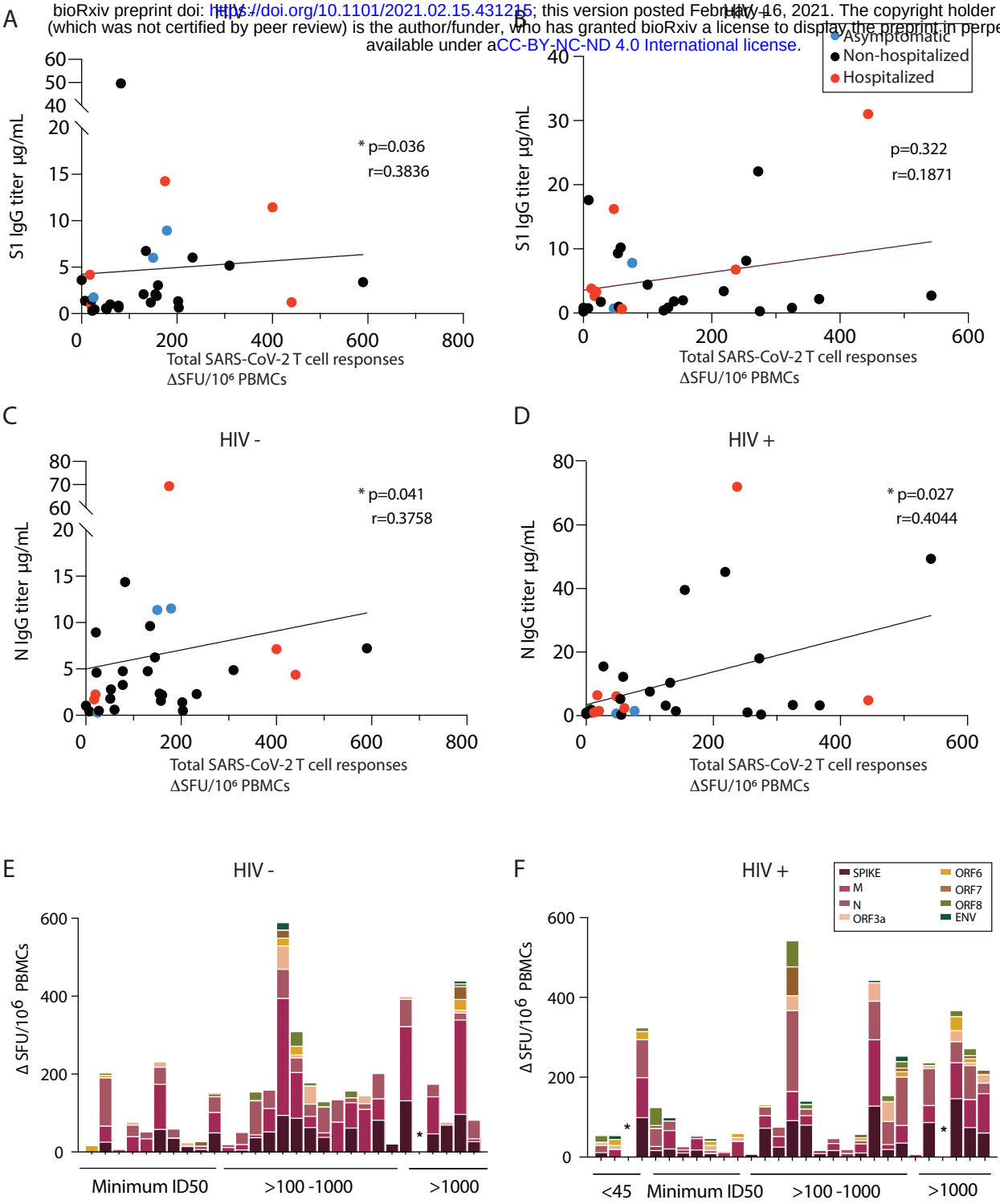

Figure 4

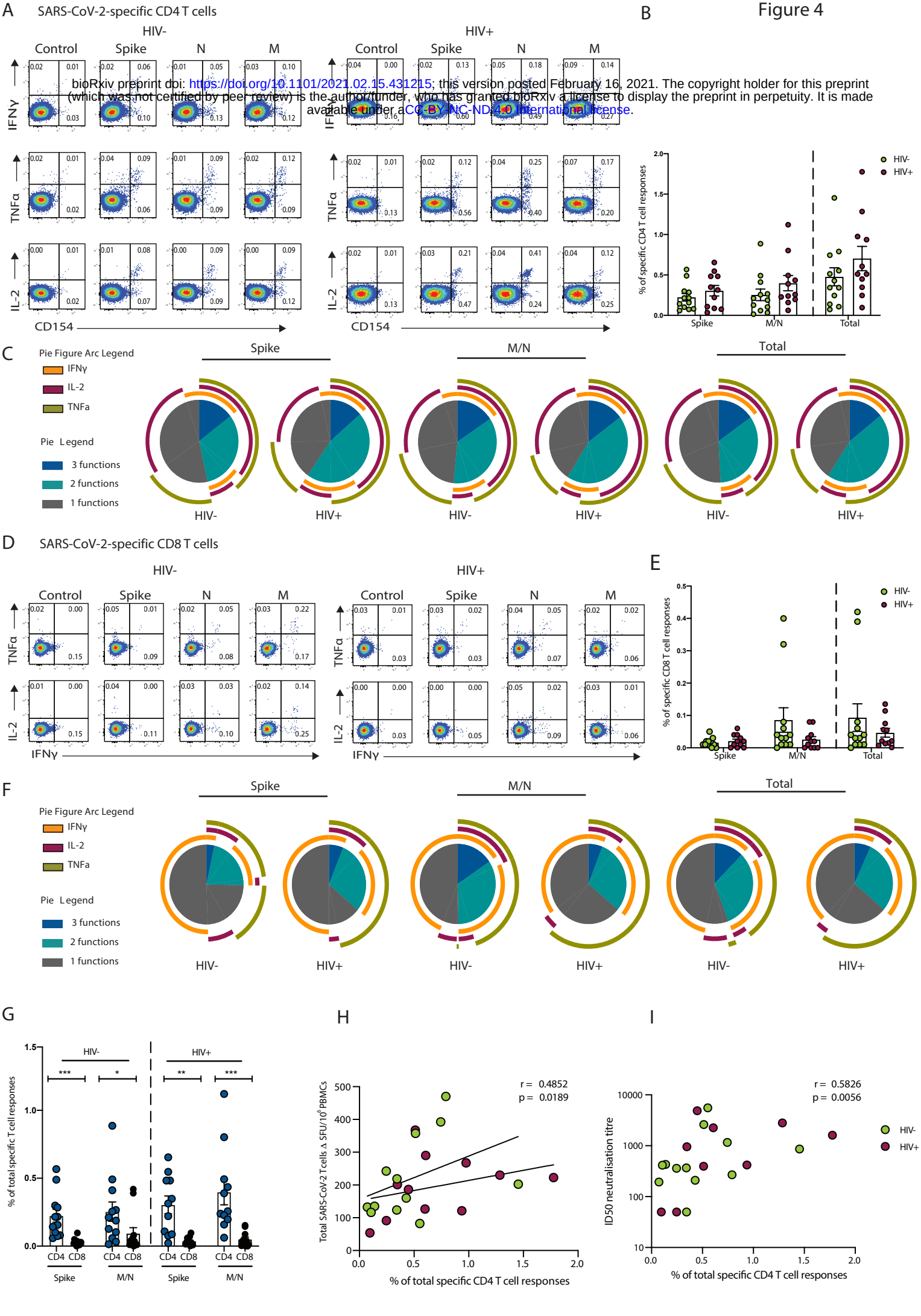

Figure 5

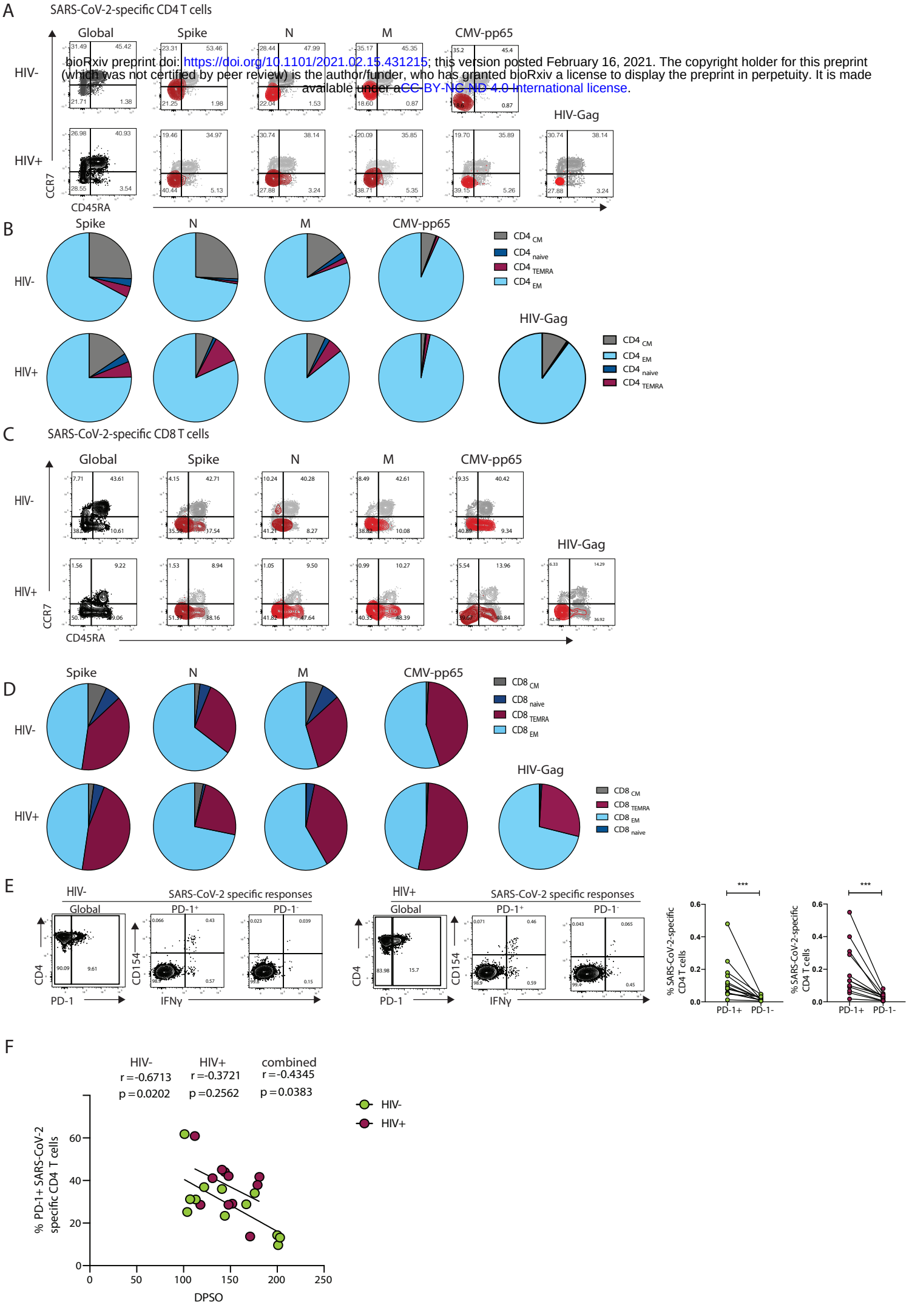

Figure 6

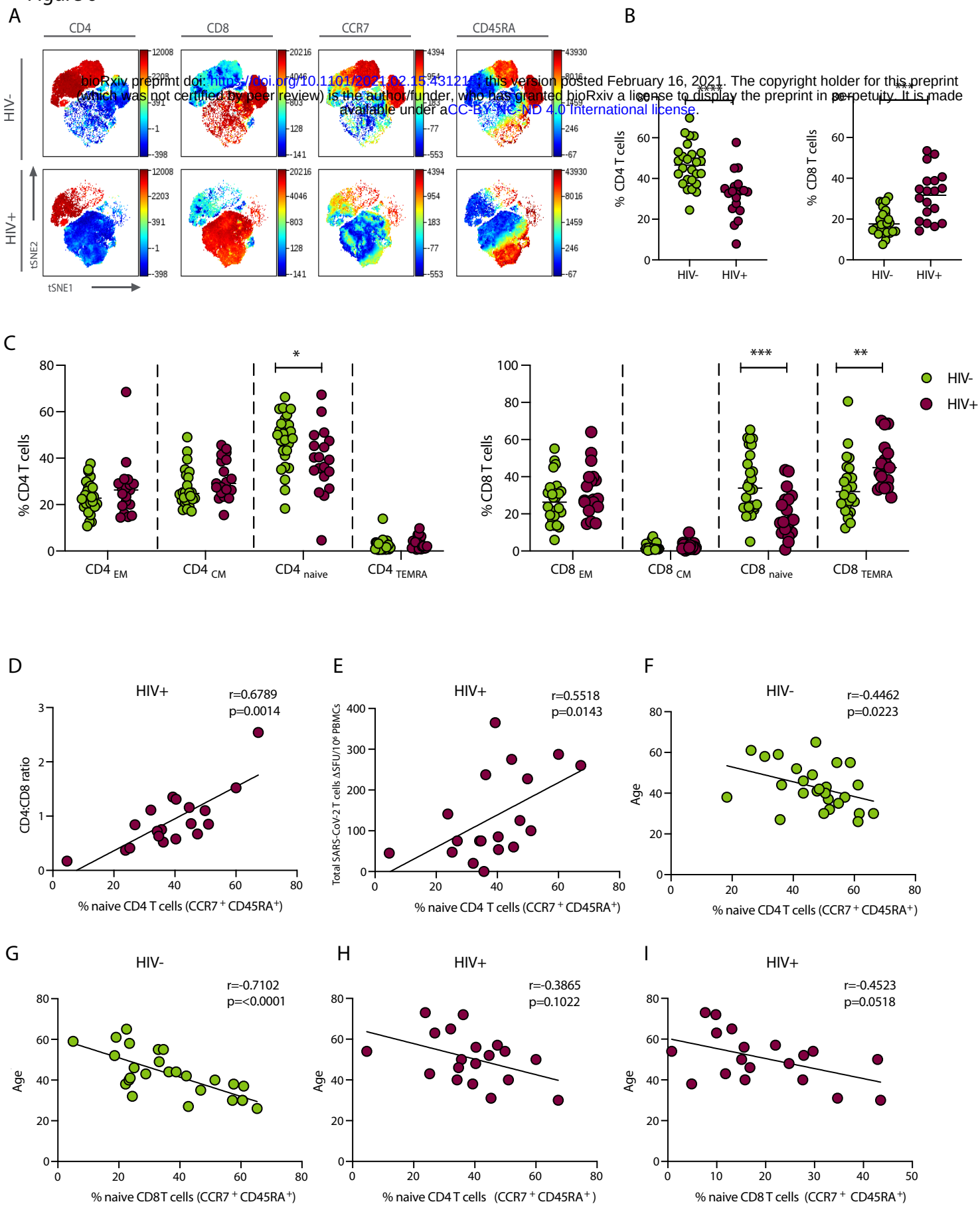

Table S1. Cohort Demographics and Clinical Characteristics

		HIV+, Lab confirmed SARS-CoV-2 RT-PCR+ and/or Ab Pos	**HIV+ *Suspected SARS-CoV-2**	**HIV- Lab confirmed SARS-CoV-2** RT-PCR+ and/or Ab Pos	**HIV- *Suspected/ Household**	**HIV+ pre-pandemic**
Group size	n	24	23	31	4	16
	SARS-CoV-2 seropositive at date of sampling, n (%)	23 (95.8)	7 (30.43)	29 (93.5)	0 (0.0)	0 (0.0)
COVID-19 severity**	Asymptomatic (score 1), n (%)	2 (8.3)	0 (0.0)	4 (12.9)	1 (25.0)	-
	Non-hospitalized (score 2), n (%)	14 (58.3)	22 (95.7)	23 (74.2)	3 (75.0)	-
	Hospitalized (score 4-5), n (%)	8 (33.3)	1 (4.3)	4 (12.9)	0 (0.0)	-
COVID-19 symptoms	Fever, n (%)	13 (54.2)	18 (78.3)	16 (51.6)	2 (50.0)	-
	Shortness of breath, n (%)	14 (58.3)	14 (60.9)	12 (38.7)	1 (25.0)	-
	Fatigue, n (%)	21 (87.5)	20 (87.0)	20 (64.5)	4 (100.0)	-
	Cough, n (%)	17 (70.8)	18 (78.3)	12 (38.7)	3 (75.0)	-
	Headache, n (%)	10 (41.7)	14 (60.9)	13 (41.9)	2 (50.0)	-
	Altered taste/smell, n (%)	13 (54.2)	10 (43.5)	22 (71.0)	2 (50.0)	-
	Duration of symptoms in days, median (range)	14 (2-48)	21 (3-84)	10 (3-30)	7 (5-7)	-
	Days post-symptom onset (DPSO), median (range)	148 (46-232)	181 (126-273)	144 (101-220)	200 (125-203)	-
Risk factors	Age, median (range)	51 (30-73)	53 (30-67)	42 (26-65)	35.5 (30-41)	48 (30-60)
	Sex, n female:male:other	4:19:1	2:21:0	16:15:0	2:2:0	2:14:0
	BMI, median (range)	27.3 (20.2-33.8)	24.6 (20.3-39.4)	25.7 (19.1-37.7)	21.9 (20.0-27.6)	
Ethnicity	White, n (%)	16 (66.7)	17 (73.9)	19 (61.3)	1 (25.0)	11 (68.8)
	BAME, n (%)	8 (33.3)	6 (26.1)	12 (38.7)	3 (75.0)	5 (31.3)
Smoking	Current, n (%)	3 (12.5)	4 (17.4)	5 (16.1)	0 (0.0)	2 (12.5)
	Ex-smoker, n (%)	1 (4.2)	1 (4.3)	2 (6.5)	0 (0.0)	1 (6.3)
	Non-smoker, n (%)	20 (83.3)	18 (78.3)	24 (77.4)	4 (100.0)	13 (81.3)
HIV parameters	HIV viral load	<50	<50	-	-	<50
	CD4, median (range)	571 (133-1110)	586 (310-1360)	-	-	590 (350-940)
	CD4:CD8, median (range)	0.84 (0.17-2.54)	0.97 (0.37-2.15)	-	-	0.82 (0.43-2.26)
Pre-existing conditions	None, n (%)	10 (41.7)	8 (34.8)	15 (48.4)	4 (100.0)	11 (68.8)
	Diabetes, n (%)	6 (25.0)	1 (4.3)	1 (3.2)	0 (0.0)	1 (6.3)
	Hypertension/CVD, n (%)	7 (29.2)	2 (8.7)	3 (9.7)	0 (0.0)	2 (12.5)
	Renal disease, n (%)	2 (8.3)	2 (8.7)	0 (0.0)	0 (0.0)	0 (0)
	Respiratory disease (asthma and COPD), n (%)	2 (8.3)	4 (17.4)	1 (3.2)	0 (0.0)	0 (0)
	Liver disease, n (%)	1 (4.2)	2 (8.7)	0 (0.0)	0 (0.0)	1 (6.3)
	Other	ITP, psoriasis, pituitary gland failure	Osteoporosis, peripheral neuropathy, hypothyroidism	RA, iron deficiency, psoriasis, gout, SLE, hypothyroidism		

*Confirmed, possible and probable cases specified by the case definition for COVID-19, as of 29 May 2020, European Centre for Disease Prevention and Control [https://www.ecdc.europa.eu/en/covid-19/surveillance/case-definition]

**Severity of COVID-19 was classified according to the WHO (World Health Organisation) clinical progression scale (Aitken et al ., 2020).

Fig. S1

A Antigen binding screen pre-2020 samples

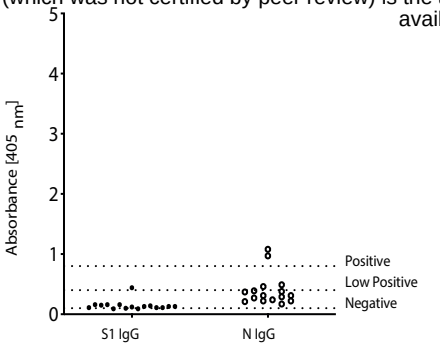

B Antigen binding screen 2020 samples

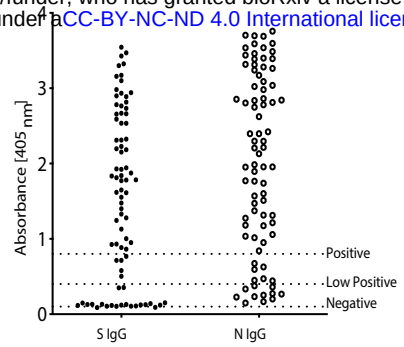

C

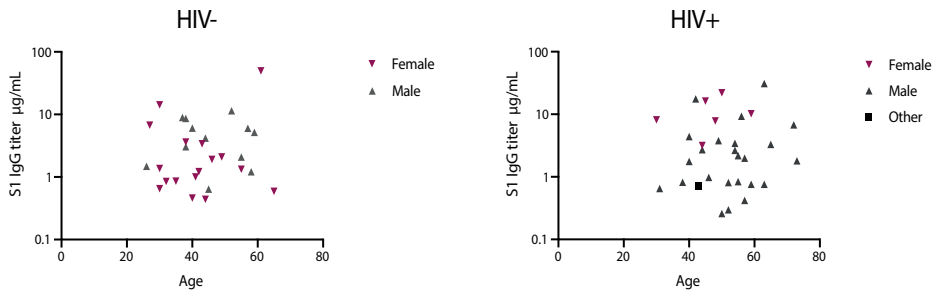

D

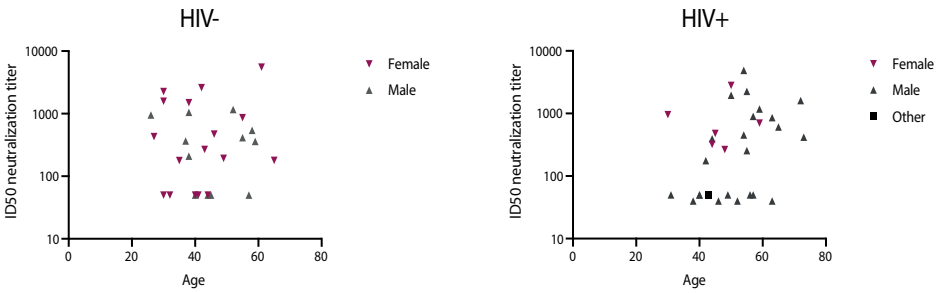

E

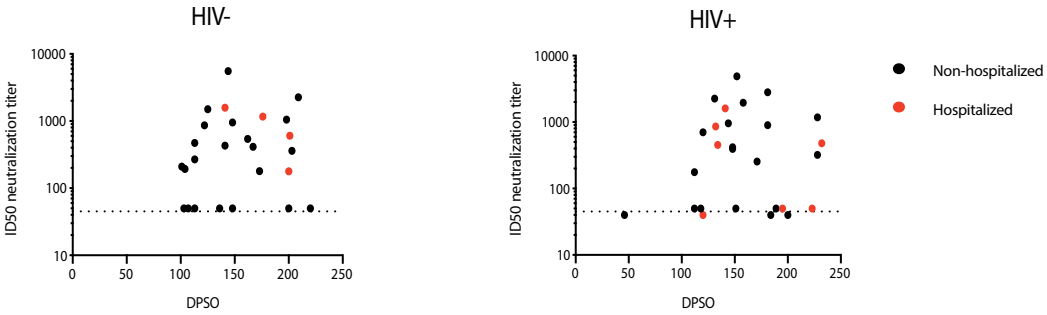

F

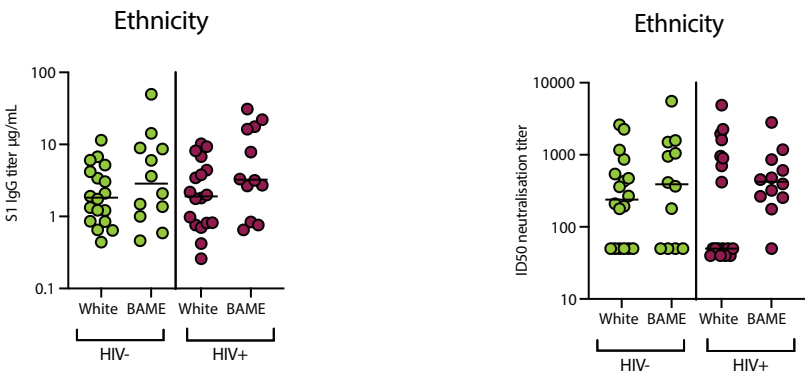

Fig. S2

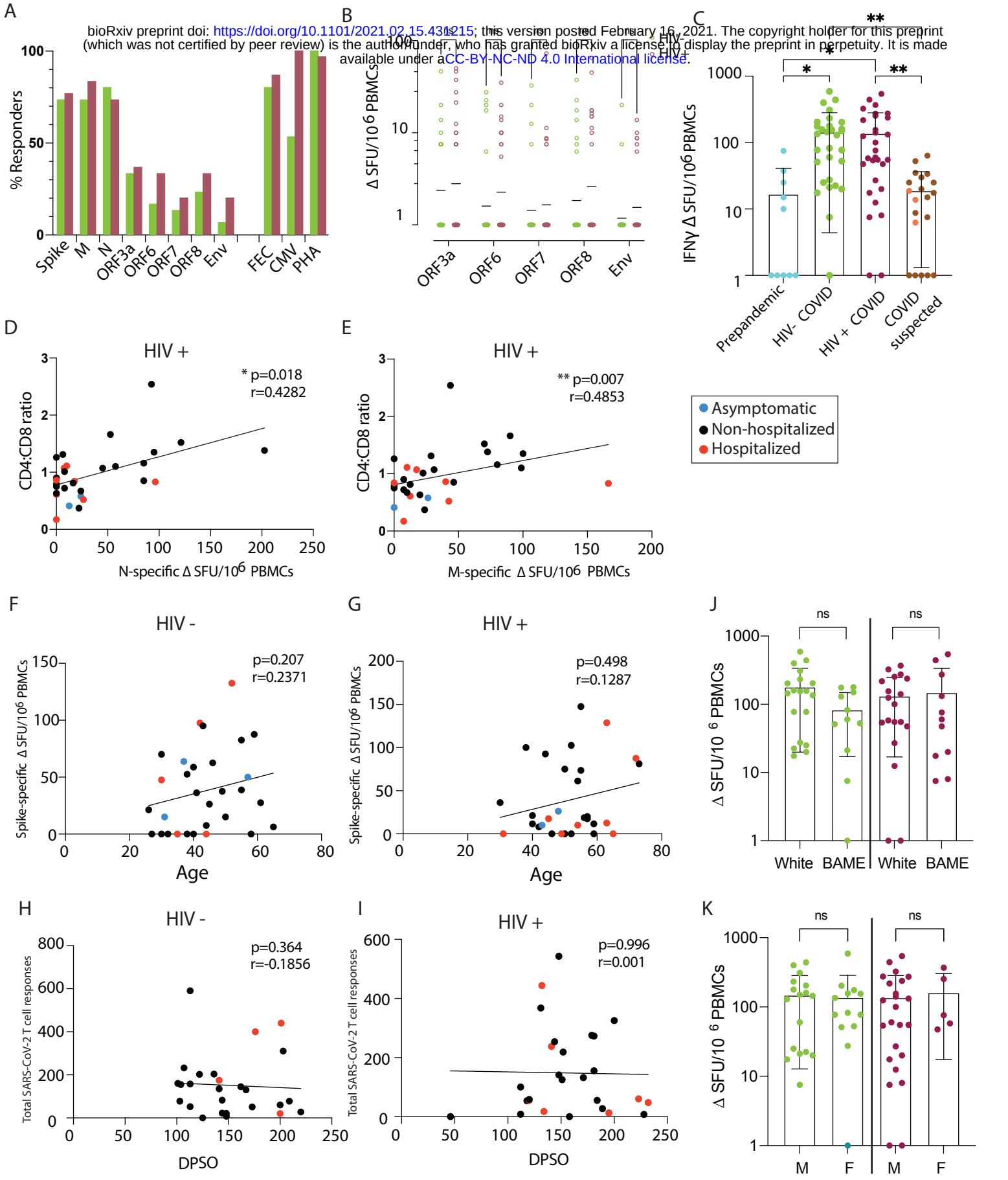

Fig. S3

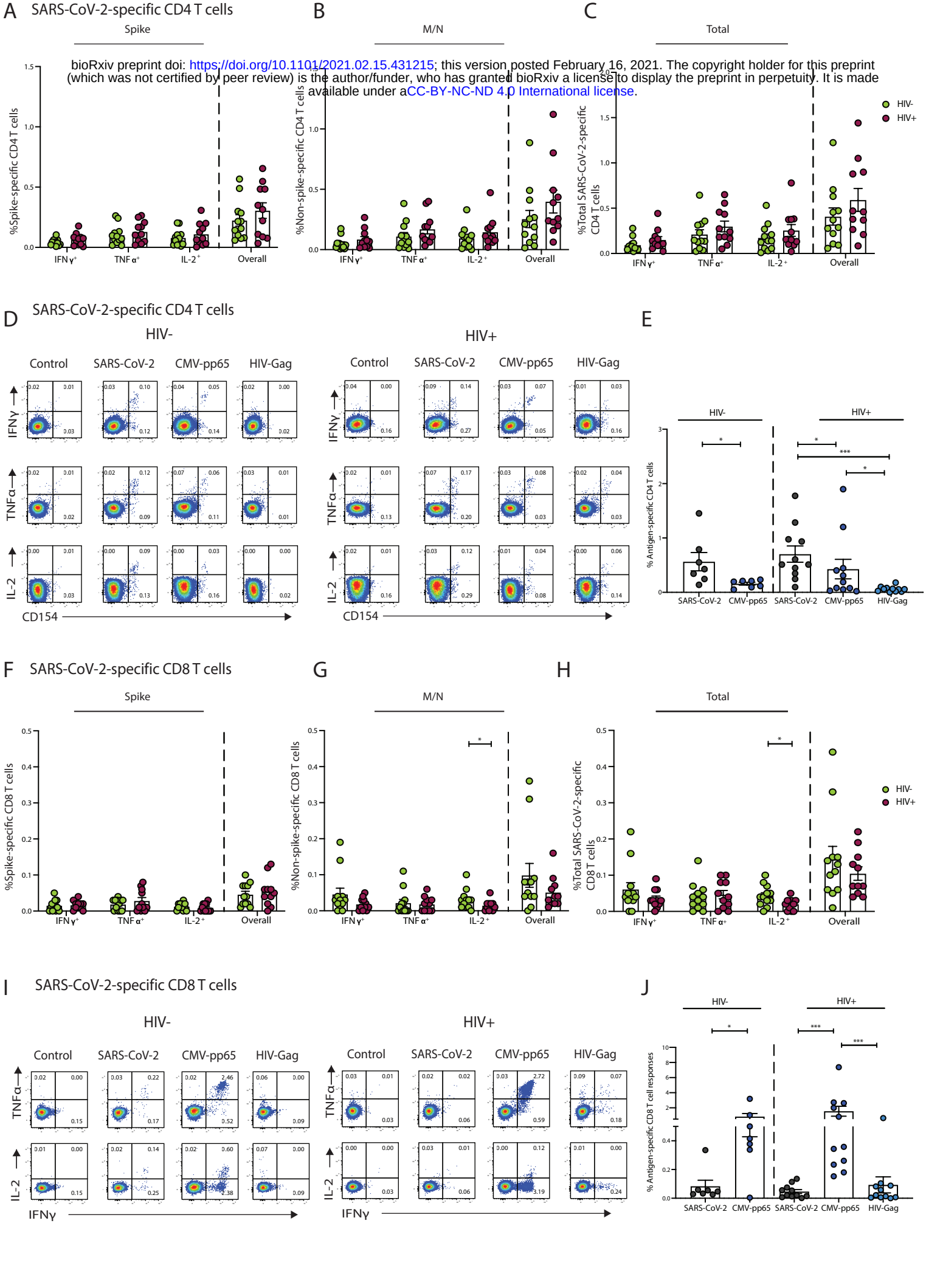

Fig. S4